

Contents lists available at ScienceDirect

Surface Science Reports

journal homepage: www.elsevier.com/locate/surfrep



Experimental and theoretical studies of reaction pathways of direct propylene epoxidation on model catalyst surfaces



William N. Porter, Zhexi Lin, Jingguang G. Chen*

Department of Chemical Engineering, Columbia University, New York, NY, 10027, USA

ARTICLE INFO

Article history: Received 28 January 2021 Received in revised form 15 March 2021 Accepted 17 March 2021 Available online 20 March 2021

Keywords: Propylene epoxidation Oxametallacycle Silver Gold Copper

ABSTRACT

The direct epoxidation of propylene to propylene oxide (PO) using molecular oxygen is an attractive alternative to current production methods using chlorohydrin or hydroperoxide-mediated processes, which are environmentally harmful and expensive. Although direct ethylene epoxidation using Ag-based catalysts has been practiced industrially for decades, due to the presence of allylic hydrogen in propylene the selectivity toward epoxide is generally much lower for propylene than for ethylene. Mechanistic understanding on well-characterized surfaces of model catalysts can potentially provide guidance to effectively alter the electronic properties of the catalyst in order to increase PO selectivity. This review summarizes both experimental and theoretical studies on model catalysts for propylene epoxidation and their contributions to elucidating the reaction mechanism, intermediates, and active sites. We first show examples of experimental studies on Cu, Ag, and Au surfaces, and compare the reaction pathways and intermediates on these surfaces. Novel approaches including plasmon-mediated catalysis and utilization of shape-controlled crystal facets that open new opportunities for improving PO selectivity will also be discussed. We then describe how density functional theory (DFT) calculations have provided important insights into the reaction mechanism and active sites on Cu, Ag, and Au surfaces and clusters. Propylene oxidation pathways on other relevant metal surfaces will also be discussed. The combined experimental and computational studies elucidate the nature of surface oxygen species and the role of the oxametallacycle intermediate. We conclude by highlighting design principles and insights for guiding further development of active and selective propylene epoxidation catalysts.

© 2021 Elsevier B.V. All rights reserved.

Contents

Introd	duction	. 2
1.1.	Unique challenges of propylene epoxidation	2
1.3.		
Comn	non techniques to study partial oxidation reactions in UHV	. 3
2.1.		
2.2.		
2.3.		
2.4.		
2.5.	Density functional theory calculations	7
Surfac		
	3.1.3. Using 1-epoxy-3-butene as a probe molecule	
	1.1. 1.2. 1.3. Comr 2.1. 2.2. 2.3. 2.4. 2.5. Surfa	1.2. Unique properties of group IB metals 1.3. Scope of the review Common techniques to study partial oxidation reactions in UHV 2.1. Surface preparation and oxidation 2.2. Temperature programmed desorption 2.3. X-ray photoelectron spectroscopy and near-edge X-ray absorption fine structure 2.4. Vibrational spectroscopy 2.5. Density functional theory calculations Surface science studies on Cu, Ag and Au surfaces 3.1. Ag surfaces 3.1.1. Using propylene as a reactant 3.1.2. Using propylene oxide as a probe molecule

E-mail address: jgchen@columbia.edu (J.G. Chen).

^{*} Corresponding author.

	3.2.	Au surfaces	11
		3.2.1. Using propylene as a reactant	11
		3.2.2. Using phenylpropene as a probe molecule	12
	3.3.	Cu surfaces	13
		3.3.1. Using propylene as a reactant	13
		3.3.2. Using propylene oxide as a probe molecule	13
		3.3.3. Using phenylpropene as a probe molecule	13
		3.3.4. Using butadiene as a probe molecule	14
	3.4.	Comparison of Cu, Ag and Au surfaces	14
	3.5.	Plasmon-mediated catalysis	15
	3.6.	Enhancing PO selectivity with shape-controlled model catalysts	16
4.	React	tion mechanism from theoretical studies on Cu, Ag and Au surfaces	
	4.1.	Ag-related surfaces	17
	4.2.	Au-related surfaces	20
	4.3.	Cu-related surfaces	
	4.4.	Comparison of Cu, Ag and Au surfaces	
5.		ies on other model surfaces	
	5.1.	Experimental studies on other surfaces	
	5.2.	Theoretical studies on other surfaces	
6.		lusions and future opportunities	
		owledgements	
	Refer	rences	24

1. Introduction

1.1. Unique challenges of propylene epoxidation

Propylene oxide (PO, also referred to as propylene epoxide) is a valuable chemical intermediate used for the production of polyurethane plastics, propylene glycol, and other chemical products [1]. Currently, the majority of PO is produced through hydroperoxide-mediated or chlorohydrin processes, which suffer from inefficiencies, hazards, and environmental costs. The organic hydroperoxide process creates coproducts with less value than PO, and the chlorohydrin process uses large amounts of chlorine and produces toxic byproducts. More recently, a process was developed using hydrogen peroxide, which remedies some of the pitfalls of the others but requires costly and hazardous H₂O₂ to be produced on-site [2]. Due to these drawbacks, direct propylene epoxidation using molecular oxygen has been proposed as an attractive alternative since such a process would be cost effective and environmentally friendly. The direct epoxidation of ethylene on Ag catalysts has been developed commercially with selectivity approaching 90% [3-10]. Nonetheless, Ag catalysts used for ethylene epoxidation cannot be easily extended to propylene epoxidation. It is generally accepted that the allylic group in propylene is more active than the C=C double bond and causes combustion to be favored over partial oxidation. The difference between these mechanisms is illustrated in a generalized reaction scheme for ethylene epoxidation and propylene epoxidation in Fig. 1. All partial oxidation products can also be further oxidized by adsorbed oxygen species to form combustion and decomposition products. Controlling the character of the adsorbed oxygen and the metal and/or metal oxide active sites is important in determining the selectivity toward these different pathways [11–13].

Research on direct propylene epoxidation has historically focused on altering the electronic properties of catalysts in order to control the basicity of the active oxygen species. Ultrahigh vacuum (UHV) experiments on single crystal metal surfaces and density functional theory (DFT) calculations have provided important mechanistic understanding. Surface science studies have reported some selectivity toward PO on group IB metal surfaces, and they have also helped elucidate the mechanism by which propylene

reacts with surface oxygen to form PO. The PO-producing pathway is generally thought to proceed through an oxametallacycle (OMC) intermediate analogous to that of ethylene epoxidation, which was first observed using a combination of UHV experiments and DFT calculations [14]. This is in contrast to the combustion pathway that goes through an allylic intermediate. Two possible configurations of the OMC intermediate in the propylene epoxidation scheme are displayed in Fig. 1(b). In the linear configuration, the methyl group is attached to the surface bound carbon atom, while the methyl group is attached to the bridging carbon in the branched configuration. Other nomenclature has been used to describe these two types of intermediates, and the specific geometry can change based on the surface; for consistency and simplicity in this review, the terms "linear" and "branched" will apply to these general categories based on the location of the methyl group. In addition to whether the OMC is in a linear or branched configuration, the number of metal atoms contributing to the ring is a factor determining the oxidation pathways. Surfaces that lower the activation barrier of OMC formation relative to the allylic intermediate and stabilize the OMC should be more selective toward epoxidation. Other partial oxidation products have been observed including acrolein and allyl alcohol. There is some debate about the pathways leading to these products, and evidence exists that different metals facilitate different pathways. For example, it has been suggested that acrolein is produced through a unique allylic oxygen insertion pathway on Au surfaces, but acrolein is generated from allylic hydrogen abstraction on Ag [11,15].

Designing a selective epoxidation catalyst is fundamentally challenging for olefins that contain allylic hydrogen atoms. Any catalyst with a propensity for non-selective oxidation is likely to favor acrolein formation and complete oxidation due to availability of the allylic hydrogen. To overcome this challenge, the formation and stabilization of the OMC intermediate should be facilitated by controlling the basicity of the adsorbed oxygen and the orientation of adsorbed propylene.

1.2. Unique properties of group IB metals

The group IB metals (Cu, Ag, and Au) are uniquely suited for the partial oxidation of propylene due to their ability to adsorb both

Fig. 1. General scheme for the partial oxidation reactions of ethylene and propylene. Minor differences in intermediate configurations and final products have been observed on different surfaces. (a) Ethylene epoxidation, (b) Selective propylene epoxidation leading to propanal, PO, and acetone formation via the (i) linear and (ii) branched OMC. (c) Allylic hydrogen abstraction leading to acrolein formation and combustion via the allylic intermediate.

oxygen and propylene, and their relatively low activity toward the complete oxidation of propylene when compared with transition metals (TM) such as Pt. All three show some extent of selectivity toward PO formation as well as other partial oxidation products. The group IB metals, with their filled d orbitals, are active for many oxidation reactions due to their ability to activate and induce negative charges on adsorbed O or OH species, often better than TMs [16]. Compared to typical TMs, they have weaker binding energy of adsorbed O and OH species. A density of states analysis by Syu et al. showed that the lower energy d-bands of the group IB metals contributed more electron density to antibonding bands of the metal-oxygen bond and, as a consequence, the p states of O had more electron density closer to the Fermi level. These higher energy p states of oxygen on Cu, Ag, and Au surfaces could more tightly bind with other atoms, leading to an increased oxidation activity. However, this enhanced activity of adsorbed oxygen species means that they are active for oxidative dehydrogenation, which is an undesirable side reaction in propylene epoxidation. Therefore, the interactions between the metal surface and the oxygen species must be controlled to achieve high PO selectivity.

1.3. Scope of the review

In this review, direct propylene epoxidation on model surfaces will be summarized with a focus on the understanding of the reaction mechanism. First, common techniques used to study partial oxidation are summarized with examples. Then, experimental studies of propylene epoxidation on single crystal surfaces of Cu, Ag, and Au are compared, along with novel approaches including plasmon-mediated catalysis and the synthesis of particles with morphology-controlled crystal facets. Following the summary of experiments on group IB metals, DFT studies are discussed in terms of insights into the reaction mechanism and active sites, both on surfaces and clusters. Finally, experimental and theoretical studies of propylene epoxidation on other metal surfaces beyond Cu, Ag, and Au are compared. The combined experimental and computational studies elucidate the nature of surface oxygen species and their interaction with the OMC intermediate. By comparing all these fundamental studies, potential design principles of active and selective propylene epoxidation catalysts are proposed, which should in turn provide insights to guide further catalyst development.

2. Common techniques to study partial oxidation reactions in $\ensuremath{\mathsf{UHV}}$

2.1. Surface preparation and oxidation

Compared with many of the more novel methods of surface synthesis and characterization that exist, the model surfaces discussed here are less complicated. Many of the studies in this review relied on oxygen modification of Cu, Ag, and Au surfaces in UHV. On Cu surfaces, oxygen readily adsorbs dissociatively. Due to the low sticking coefficient of oxygen on Ag and Au surfaces, several different techniques have been employed to prepare oxygen-covered surfaces or metal oxide structures. Methods to prepare atomic oxygen included exposing the surface to ozone [17], dissociation of molecular O_2 over a hot W filament, or electron bombardment following exposure to NO_2 [18]. A more detailed list of the methods for atomic oxygen preparation on Au surfaces was presented by Min et al. [19]. In addition to these methods of surface oxidation, lengthy exposures $(1 \times 10^{-6}$ Torr for 60 min [20], for example) were used to facilitate the propylene epoxidation reaction by co-dosing propylene and oxygen in UHV.

On Cu(110), Cu(100), and Ag(110) surfaces, oxidation leads to the formation of mobile surface rows of alternating metal and oxygen atoms along the [001] direction, which agglomerate into (2×1) or $c(6 \times 2)$ structures at saturation coverage [11,21]. On Au, oxidation is quite complex and metastable herringbone surface structures are formed depending on the oxidation conditions. This leads to Au or Au-O island formation on the surface, where chemisorbed oxygen is present [19]. Beyond a critical coverage and if the corresponding activation barrier is exceeded, bulk oxidation occurs via growth of surface oxide islands. Bulk Cu₂O and CuO structures are readily formed on Cu surfaces in UHV, while ordered bulk Ag and Au oxides are less stable. The interaction of oxygen with metal surfaces plays a vital role in the PO selectivity and intermediate stabilization. Several groups have studied these interactions in the context of partial oxidation reactions with a focus on the electronic properties of the active oxygen species [18,21–25].

2.2. Temperature programmed desorption

Temperature programmed desorption (TPD, also referred to as temperature programmed reaction) has been used extensively in model surface studies relevant to propylene epoxidation. TPD allows identification and quantification, via mass spectrometry, of the gas phase products desorbing from a surface following

adsorption of a controlled dose of the molecule of interest. In a typical TPD experiment, a prepared surface is exposed to a known amount of reactants, followed by a ramp of surface temperature at a linear heating rate within a desirable range necessary for product desorption. In this process, the identity, amount, and binding strength of the product can be determined. Hence, TPD is an effective and powerful technique for probing surface reactions. Furthermore, when TPD is combined with electron spectroscopy and vibrational spectroscopy, reaction mechanisms can often be clearly determined.

Discussed below are two examples of TPD experiments that assisted in product identification and quantification. Yang et al. used the TPD method to detect the desorbed products after dosing propylene and oxygen to the corresponding surfaces (Cu(111), Cu₂O, and TiCuO_X with different coverages of TiO_X) [20]. Fig. 2(a) shows the desorption of the cracking fragments of PO with m/ e = 43, 31, 58, 56. The concurrent detection of such desorption peaks confirmed the formation and desorption of PO. Fig. 2(b) compares the amount of PO produced on the corresponding surfaces on the same scale, revealing that the TiCuO_X surface with 0.6 ML TiO_X had the highest PO yield and suggesting that the TiO_X/ Cu₂O interface enhanced the PO production.

In another example, Liu et al. used the TPD method to probe the desorption products after exposing an oxygen-covered Au(111) surface to trans-β-methylstyrene, which is a model compound for studying the epoxidation reactions of allylic olefins [26]. Fig. 3 shows that the epoxidation product, trans-β-methylstyrene oxide (m/z = 134) was detectable on surfaces with different oxygen coverages. While only one trans-β-methylstyrene oxide desorption peak was observed on 0.2 ML O/Au(111), two were observed on 1 ML O/Au(111), suggesting that there were two kinetically distinct processes. The product distribution also changed as oxygen coverage increased. Cinnamic acid (m/z = 148) desorption was detected on 0.2 ML O/Au(111), but not on 1 ML O/Au(111). In contrast, as oxygen coverage increased from 0.2 ML to 1 ML, the desorption peak of benzoic acid (m/z = 122) broadened and shifted to a higher temperature. In addition, substantially more CO₂ and H_2O were formed on 1 ML O/Au(111) than on 0.2 ML O/Au(111). The

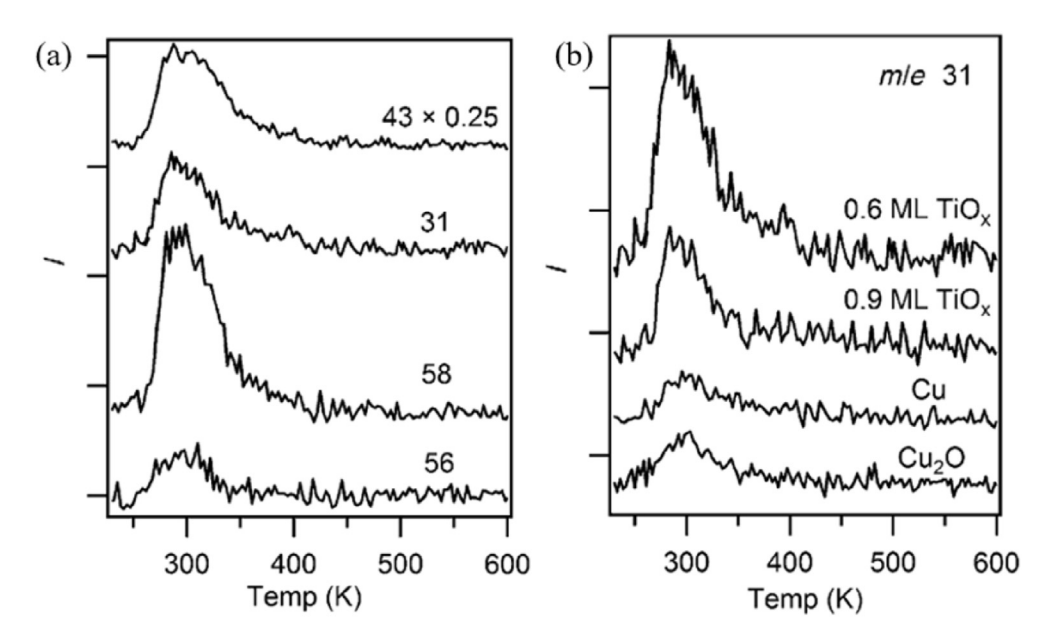
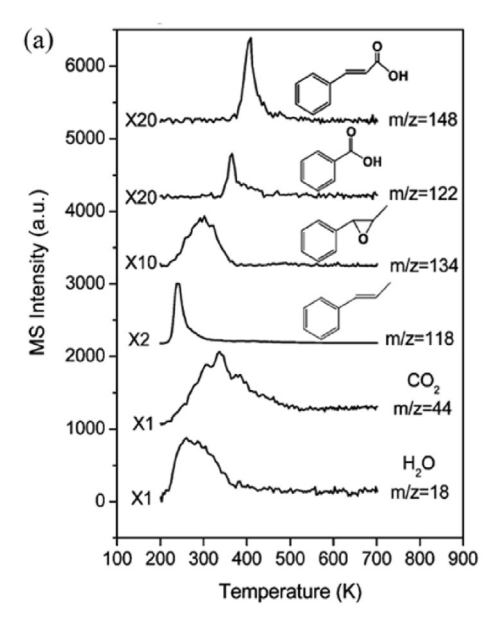


Fig. 2. TPD of propylene epoxidation on (a) TiCuO_X, for the m/e values indicated next to the traces (the m/e = 43 peak is scaled by 0.25) and on (b) Cu₂O, Cu(111), and 0.9 ML and 0.6 ML of TiO_X. The epoxidation conditions were 1.0×10^{-6} Torr of O₂ and 1.0×10^{-6} Torr of propylene at 240 K for 60 min. Reprinted with permission from Yang et al. [20]. © 2015 Wiley-VCH Verlag GmbH & Co.



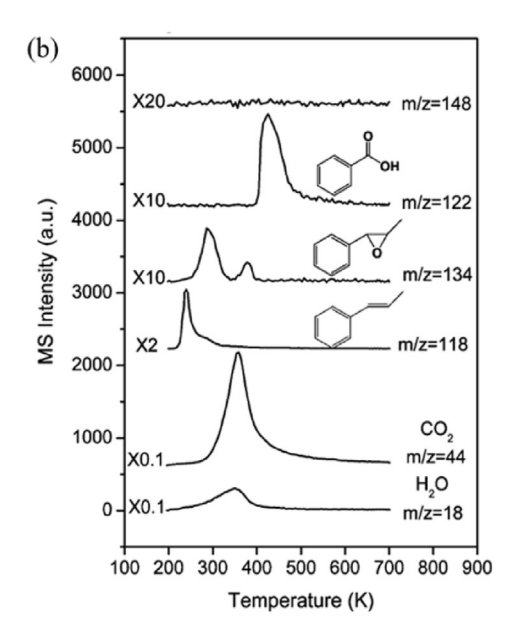


Fig. 3. TPD of trans- β -methylstyrene on oxygen-covered Au(111) with (a) 0.2 ML and (b) 1 ML of oxygen coverage. Signals of the parent ions of water (m/z = 18), CO₂ (m/z = 44), trans- β -methylstyrene (m/z = 118), trans- β -methylstyrene oxide (m/z = 134), benzoic acid (m/z = 122), and cinnamic acid (m/z = 148) are shown. Reprinted with permission from Liu et al. [26]. © 2010 American Chemical Society.

common peak temperature for CO_2 and H_2O on 1 ML O/Au(111) also suggested there was a common rate-limiting step for complete oxidation. Based on the results provided in the examples, it is clear that much information can be obtained from TPD experiments, which provide a basis for further study of surface intermediates and reaction mechanisms.

2.3. X-ray photoelectron spectroscopy and near-edge X-ray absorption fine structure

X-ray photoelectron spectroscopy (XPS) is an essential surface science tool that allows determination of elemental surface composition and metal oxidation state. It is a surface sensitive technique that relies on excitation of electrons using an X-ray photon beam, followed by energy-specific detection of the emitted electrons. For studying the propylene epoxidation reaction, XPS is particularly useful because it can be used to identify changes in the local binding environment of surface atoms. For example, the OMC intermediate has been identified through changes in the C(1s) spectra following PO adsorption at different temperatures [20].

An example by Cropley et al. is shown in Fig. 4 [27]. In this study, synchrotron based temperature programmed fast XPS was used to identify the oxidation states of the oxygen species on Cu(111) after dosing oxygen and trans-methylstyrene in different orders. Fig. 4(a) and (c) show the XP spectra of the surfaces with different dosing sequences. Comparing these two figures, both adsorbed hydroxyl group (531.2 eV) and adsorbed oxygen (528.6 eV) were present. The adsorbed hydroxyl group was likely a result of allylic hydrogen stripping (AHS). The adsorbed oxygen consisted of isolated oxygen species that were active for epoxidation, and oxidic oxygen that was ineffective for epoxidation. Additionally, a distinct peak at 528.9 eV was observed on the trans-methylstyrene pre-dosed surface but not on the oxygen pre-dosed surface. This oxygen species was designated as a metastable oxygen species, which was converted into atomic oxygen upon heating, as evidenced by the simultaneous decrease in its intensity and increase in the atomic oxygen intensity (Fig. 4(b)). It was speculated that the pre-adsorbed trans-methylstyrene forced oxygen to adsorb on the interstices in the trans-methylstyrene layer, and prevented the growth of oxidic oxygen islands, leading to higher selectivity in epoxide formation. As the temperature was increased to 500 K, all the oxygen species had been consumed. By tracking the evolution of the surface oxygen species with XPS, the authors were able to understand the dynamic changes in surface intermediates and thereby elucidate the reaction mechanism.

Another electron spectroscopy that has been employed for propylene epoxidation is near-edge X-ray absorption fine structure (NEXAFS), in particular at the C and O K-edge region. By measuring the dipole transitions of the C(1s) or O(1s) electrons to the unoccupied orbitals, the K-edge NEXAFS results provide information to differentiate different types of surface adsorbates and intermediates, as well as their orientation on the surface [28,29]. As discussed later, this technique has been utilized in several studies to help identify the surface intermediates and reaction pathways of propylene epoxidation.

2.4. Vibrational spectroscopy

High-resolution electron energy loss spectroscopy (HREELS) and reflection absorption infrared spectroscopy (RAIRS) are vibrational spectroscopic techniques that aid in the identification of surface intermediates and reaction mechanisms. By means of the energy loss of inelastically scattered electrons, or absorption in a reflected IR beam, respectively, these methods allow observation of the vibrational modes present on a model surface. Details about adsorption geometry can be determined through the selection rules of these techniques. While RAIRS has a higher spectroscopic resolution (4 cm⁻¹), HREELS typically has higher sensitivity and a wider spectral range (100 - 4000 cm⁻¹), and can perform offspecular measurements to identify modes parallel to the surface. Coupled with knowledge of the desorption temperatures of reaction products from TPD, vibrational spectra measured after heating to different temperatures can be used to determine the surface intermediates that lead to the formation of certain products. In addition, other mechanistic details, such as the occurrence of hydrogen abstraction, can be determined by the detection of

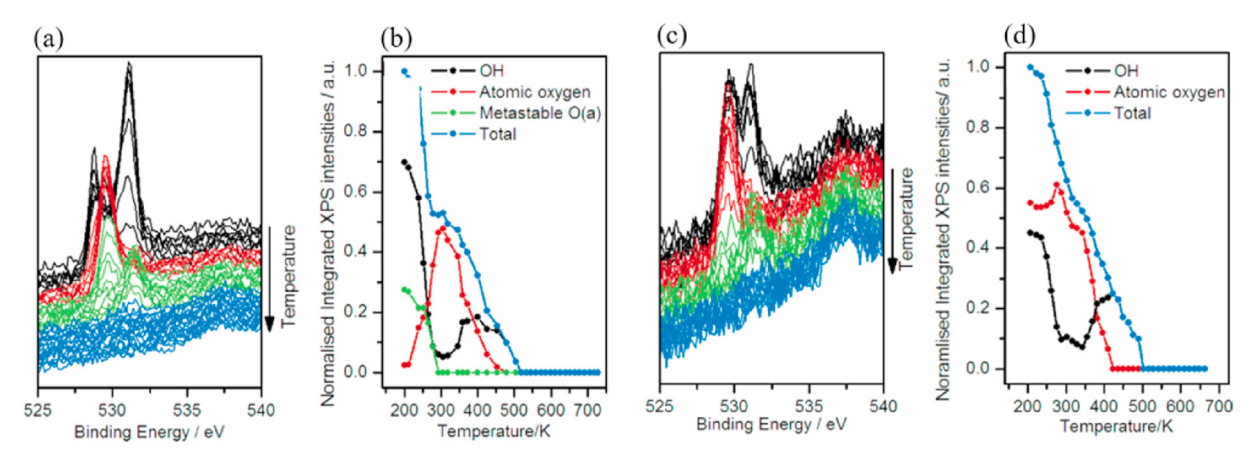


Fig. 4. (a) O(1s) fast XP spectra showing products from 0.07 ML oxygen exposed to 0.07 ML pre-adsorbed trans-methylstyrene on Cu(111). (b) Integrated intensities of species observed in (a) vs. Temperature. (c) O(1s) fast XP spectra showing products from 0.04 ML trans-methylstyrene dosed to 0.04 ML of pre-adsorbed oxygen on Cu(111). (d) Integrated intensities of species observed in (c) vs. Temperature. Reprinted with permission from Cropley et al. [27]. © 2005 American Chemical Society.

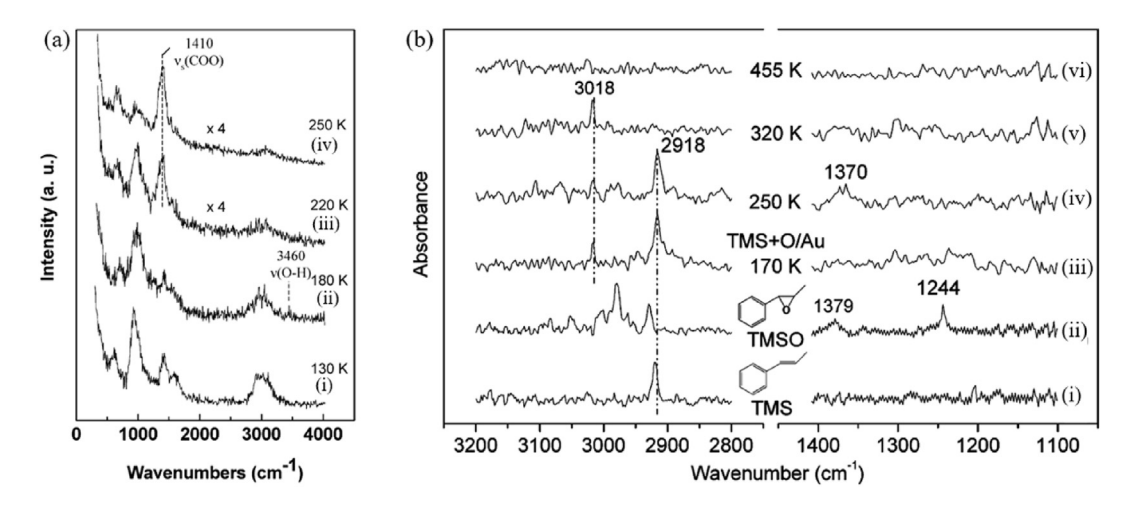


Fig. 5. (a) HREEL spectra of (i) propylene adsorbed on 0.3 ML oxygen-covered Au(111) at 130 K, and after heating to (ii) 180, (iii) 220, and (iv) 250 K. (b) RAIRS of (i) 1 ML trans-β-methylstyrene on Au(111), (ii) 1 ML trans-β-methylstyrene on Au(111), at (iii) 170 K, followed by annealing to (iv) 250 K, (v) 320 K, and (vi) 455 K. (a) Reprinted with permission from Deng at al [30]. © 2006 American Chemical Society. (b) Reprinted with permission from Liu et al. [26]. © 2010 American Chemical Society.

characteristic vibrational modes.

Shown in Fig. 5(a) is an example of using HREELS to identify important surface intermediates by Deng et al. [30]. The authors dosed propylene to an oxygen pre-dosed Au(111) surface at 130 K, annealed the surface to specific temperatures, and measured the corresponding HREEL spectra. As shown in Fig. 5(a)(ii), the ν (OH) feature at 3460 cm⁻¹ was detected, indicating the activation of allylic hydrogen by atomic oxygen to produce the –OH group. After further heating to 220 K, the ν s(COO) feature at 1410 cm⁻¹ appeared, suggesting the formation of acrylate species, which was an intermediate of partial oxidation products. The HREELS results together with TPD data allowed the authors to propose the reaction mechanism.

Fig. 5(b) demonstrates an example of using RAIRS to monitor the surface intermediates. In this example, Liu et al. measured a thermal sequence (Fig. 5(b)(iii-vi)) after exposing O/Au(111) to trans-β-methylstyrene, and compared the spectra to two reference spectra (trans-β-methylstyrene (Fig. 5(b)(i)) and trans-β-methylstyrene oxide (Fig. 5(b)(ii)) on Au(111)) [26]. The trans-β-methylstyrene oxide ring feature at 1244 cm⁻¹ (Fig. 5(b)(ii)) was not detected at any temperature in the thermal sequence. Since the corresponding

TPD results suggested the desorption of trans-β-methylstyrene oxide (shown in Fig. 3), this indicated that the desorption of the epoxide was reaction limited (i.e. the product desorbed as soon as it was formed and was therefore not detectable by RAIRS). In addition, the different vibrational frequencies of the C-H stretching mode of trans-β-methylstyrene oxide (Fig. 5(b)(ii)) and the intermediate from the thermal sequence (2918 cm⁻¹, Fig. 5(b)(iii-iv)) also support this argument. According to the surface dipole selection rule, the absence of the (-C-H) stretching mode in the thermal sequence suggested that the ring and the vinyl group were parallel to the surface. After heating the surface to 250 K, a new feature at 1370 cm⁻¹ appeared, which likely indicated the formation of benzoate or cinnamate intermediates, consistent with the desorption of benzoic and cinnamic acid in the TPD experiments (Fig. 3). Upon heating the surface to 320 K, only one feature at 3018 cm⁻¹ remained, corresponding to the C-H stretching mode in the phenyl group of the benzoate or cinnamate intermediate, or other hydrocarbon residues on the surface. After heating to 455 K, all adsorbed species had desorbed from the surface, consistent with the TPD results (Fig. 3). This example illustrates the feasibility and effectiveness of using RAIRS to capture the evolution of surface

intermediates and identify the adsorption orientation of specific surface species. The combination of TPD, XPS, and HREELS/RAIRS provides a clear picture of gas phase products as well as surface intermediates, which is essential for understanding the reaction mechanism.

2.5. Density functional theory calculations

Density functional theory (DFT) calculations have been shown to be very important in elucidating reaction mechanisms relevant to propylene epoxidation. DFT calculations are used to investigate the ground state electronic structures of both the adsorbate and the catalytic material by numerically solving the Kohn-Sham equation [31]. After establishing an appropriate model, DFT can be used to calculate the adsorption energy, activation barrier of elementary reaction, and charge density of the system, among others [32,33]. Such information can be used to help explain experimental observations and provide additional insights into the reaction mechanism. Output from DFT calculations can also be used as input for microkinetic modeling or kinetic Monte Carlo simulations to predict catalytic performance under realistic conditions [34].

Shown in Fig. 6 is an example by Düzenli et al. that used DFT to investigate the adsorption energies and configurations of propylene epoxidation intermediates on $Cu_2O(001)$ and CuO(001), as well as the activation energies of critical elementary reactions [32]. Fig. 6(a-b) compare two possible OMC intermediates on $Cu_2O(001)$. In the linear structure, propylene was bound to an oxygen atom via C1 and a copper atom via C2. The proximity of the allylic hydrogen and the nearby bridge oxygen atom favored AHS, rendering the linear structure to be unstable. On the other hand, the branched structure with the methyl group tilted away from the surface was calculated to be formed without any barrier. Therefore, only the branched structure was suggested as an intermediate to PO formation. On CuO(001), a stable intermediate of chemisorbed

propylene (labeled as the oxygen bridging (OB) intermediate) was obtained with a barrier of 0.52 eV, with a structure in which both C1 and C2 were bonded to oxygen atoms. The authors further compared the energy profiles on Cu₂O(001) and CuO(001) and found that on Cu₂O(001), PO formation was more kinetically favorable by 0.13 eV, while the AHS pathway to form acrolein was more thermodynamically preferred (Fig. 6(d)). In contrast, on CuO(001), the allyl radical readily produced acrolein, while the OB intermediate had to overcome an activation barrier greater than 2.5 eV to form PO. The high selectivity to acrolein on CuO(001) was attributed to the more basic nature of the oxygen species on CuO(001), which promoted the stripping of the allylic hydrogen of propylene. Overall, in this example, the authors used DFT calculations to study the adsorption energies and geometries of important reaction intermediates, as well as the activation barriers of critical elementary reactions to gain an in-depth understanding of the reaction mechanism of propylene epoxidation over Cu₂O(001) and CuO(001), which helped to explain the selectivity difference between the two surfaces.

3. Surface science studies on Cu, Ag and Au surfaces

Group IB metal catalysts are the most promising materials for propylene epoxidation, and a detailed review of studies over powder catalysts has been provided by Huang and Haruta [35] in 2012. Various supports, alloys, and promoters have been used to improve selectivity and conversion, but understanding their effects relies on insights about the mechanism and active sites for propylene epoxidation. The following sections review experimental studies on model group IB metal catalytic surfaces; results on most commonly studied Ag surfaces are discussed first, followed by results on Au and Cu. All the work to be reviewed in this section is summarized in Table 1.

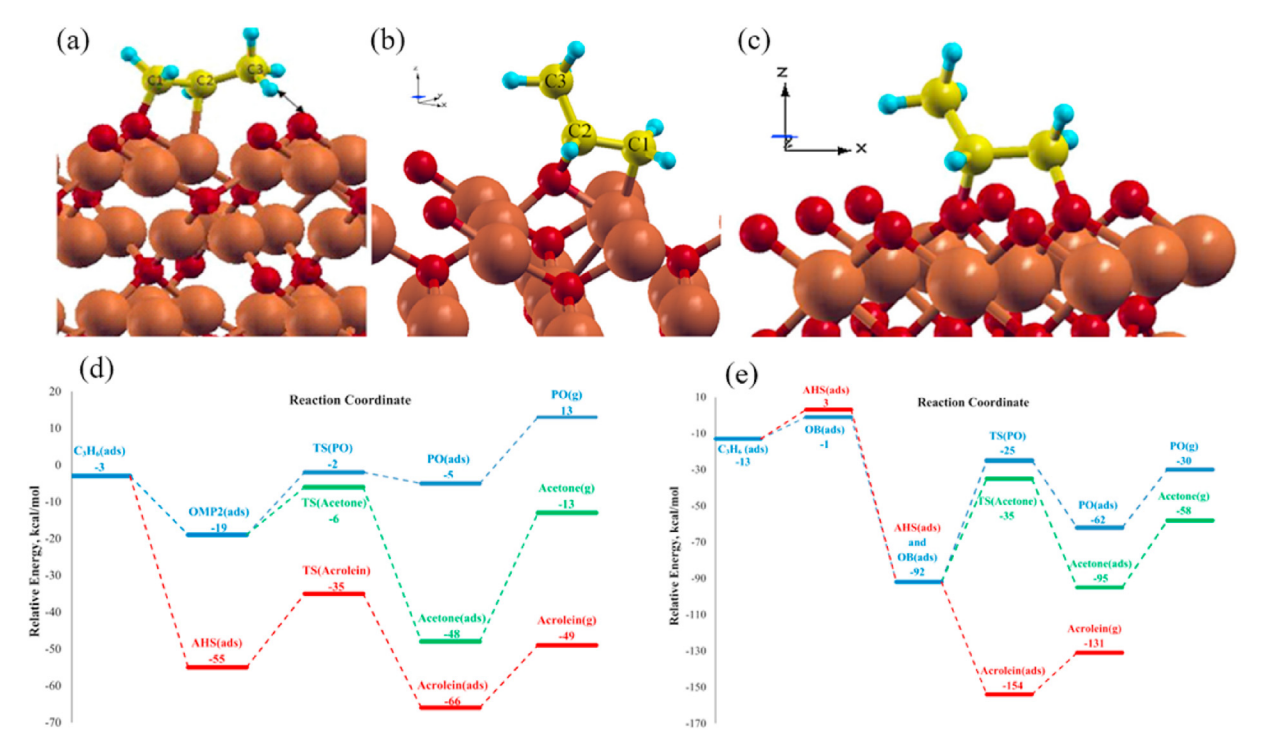


Fig. 6. (a) Linear (OMP1) and (b) branched (OMP2) geometries on $Cu_2O(001)$. (c) Geometry of propylene on CuO(001). (d) Energy profiles for propylene epoxidation on (d) $Cu_2O(001)$ and (e) CuO(001). Reprinted with permission from Düzenli et al. [32]. © 2015 Elsevier. B.V.¹¹

Table 1UHV studies related to propylene epoxidation.

Reactants	Surfaces	Techniques
propylene	Au(111)	TPD, HREELS, LEED [36]
propylene	O/Au(111)	TPD, HREELS, LEED [30,36]
propylene	Au(100)	TPD, HREELS, LEED [36]
propylene	O/Au(100)	TPD, HREELS, LEED [36]
propylene	O/Au(997)	TPD, PM-RAIRS [37]
trans-methylstyrene	Au(111)	TPD, RAIRS [26]
trans-methylstyrene	O/Au(111)	TPD, RAIRS [26]
propylene	Ag(111)	TPD, RAIRS [38-40], Raman [15]
propylene	O/Ag(111)	TPD, RAIRS [38,40,41]
propylene ^a	O/Ag(100)	MS, Raman [15]
propylene	O/Ag(110)	TPD [42-45]
propylene	OH/Ag(110)	TPD [46]
propylene oxide	Ag(110)	NEXAFS [47]
propylene oxide	Ag(110)	TPD, HREELS, LEED, XPS [48]
propylene oxide	O/Ag(110)	TPD [46,48], HREELS, LEED, XPS [48]
1-epoxy-3-butene	Ag(110)	TPD, HREELS [49], NEXAFS [50]
propylene	Cu ₂ O/Cu(111)	AES, XPS, TPD [51]
propylene	CuO/Cu(111)	AES, XPS, TPD [51]
propylene	Cu ₂ O(100)	TPD, LEED, XPS [52,53], UPS [53]
propylene	Cu ₂ O(111)	TPD, LEED, XPS [52,53], UPS [53]
propylene ^a	O/Cu ₂ O(100)	TPD, LEED, XPS [52]
propylene ^a	O/Cu ₂ O(111)	TPD, LEED, XPS [20]
propylene + oxygen	TiCuO _x	TPD, HREELS, XPS [20]
propylene + oxygen	Cu ₂ O	TPD, HREELS, XPS [20]
propylene + oxygen	Cu(111)	TPD, HREELS, XPS [20]
propylene oxide	TiCuO _x	TPD, HREELS, XPS [20]
propylene oxide	Cu ₂ O	TPD, HREELS, XPS [20]
propylene oxide	Cu(111)	TPD, HREELS, XPS [54]
phenylpropene isomers	Cu(111)	TPD [37,54], NEXAFS [27,55]
trans-methylstyrene + oxygen	Cu(111)	TPD, NEXAFS [27], XPS [56]
butadiene	O/Cu(111)	TPD, XPS [57]
propylene	Au/TiO ₂	TPD, XPS, LEIS [58]
propylene	TiO ₂ (110)	TPD [59]
propylene oxide	Rh(111)	TPD, HREELS [60]
propylene	Rh(111)	TPD [61]
propylene	Pt(111)	TPD [62], NEXAFS [62]

^a Single crystal surface at atmospheric pressure.

3.1. Ag surfaces

3.1.1. Using propylene as a reactant

Initial studies of propylene epoxidation with molecular oxygen focused on Ag-based catalysts due to the successful use of supported Ag for the gas phase epoxidation of ethylene. Barteau and Madix [43] observed 100% selectivity for combustion to produce CO₂ and H₂O on Ag(110), and found that the abstraction of allylic H atoms was an important step in the combustion mechanism. Their comparison of propylene and ethylene supported the importance of acid-base properties for partial oxidation processes, with propylene being more reactive toward hydrogen abstraction than ethylene on the oxygen-covered Ag(110) surface. By titrating the propylene- and oxygen-covered surface with acetic acid after heating to different temperatures and observing the surface acetates formed, the authors concluded that the reaction produced only adsorbed carbon and hydroxyl groups.

Pawela-Crew and Madix [45] observed that subsurface oxygen had very little effect on propylene adsorption on the Ag(110) surface, although this study did not investigate the effect of subsurface oxygen on surface oxygen species. It has been shown that subsurface oxygen could promote surface oxygen activity toward ethylene epoxidation by weakening the bond between the surface and chemisorbed oxygen, thus making the ethylene-oxygen interaction

more facile [63]. In addition, theoretical studies have shown the ability of subsurface oxygen to improve the kinetics of oxygen dissociation on Ag(111) [23].

In a study of propylene oxidation on Ag(110), Roberts et al. [42] found that the rate-determining step of propylene combustion was C—H bond activation through an acid-base reaction with adsorbed oxygen, and combustion proceeded via abstraction of the allylic hydrogen by surface atomic oxygen. TPD results for oxygen coverages ranging from 0.05 to 0.5 ML showed only desorption of unreacted propylene, CO_2 , and H_2O . In their proposed mechanism, after stripping of this allylic hydrogen by surface oxygen species, the allylic intermediate rapidly combusted and then a disproportionation reaction between two adsorbed hydroxyl groups occurred to produce water and adsorbed oxygen.

Further investigation of the effect of different oxygen species on Ag(110) revealed that disordered surface oxygen atoms were more reactive than the ordered Ag–O row structures formed from higher temperature exposure [44]. In particular, for propylene reacting with 0.33 ML oxygen adsorbed at 183 K, large amounts of CO_2 and H_2O desorption were observed. In comparison, with 0.35 ML oxygen adsorbed at 478 K, much lower yields of combustion products were observed. The authors attributed this difference to much shorter, more disordered Ag–O chains formed at the lower adsorption temperatures, which had higher oxidation rates due to the increased concentration of terminal oxygen atoms.

Huang et al. [38,41] studied the adsorption geometry of propylene on Ag(111) using TPD and RAIRS, and it was found that propylene adsorbed with the C=C bond parallel to the surface in a weakly π -bonded configuration. In a separate study of propylene

¹ Reprinted from Publication title, Vol /edition number, Author(s), Title of article / title of chapter, Pages No., Copyright (Year), with permission from Elsevier [OR APPLICABLE SOCIETY COPYRIGHT OWNER].

oxidation on Ag(111), they observed a transition from π -bonded to di- σ -bonded propylene with increasing oxygen coverage, and RAIRS results indicated that π -bonded propylene underwent combustion via AHS while di- σ -bonded propylene underwent a different combustion mechanism [38]. The authors also reported some selectivity toward acetone formation, indicating that the surface had partial oxidation capability, but not toward PO formation. Increased intensity of the water desorption peak when acetone was observed indicated that acetone was further oxidized to form combustion products. Fig. 7 displays the vibrational spectra of propylene on O/Ag(111) annealed to different temperatures. The peak at 3567 cm⁻¹ was attributed to a hydroxyl group formed from abstraction of allylic hydrogen by surface oxygen. At all three coverages, it appeared coincidently with the disappearance of the

characteristic hydrocarbon peaks, indicating that the adsorbed propylene decomposed significantly upon losing this hydrogen. These results were consistent with a combustion mechanism on Ag(111) that was initiated by abstraction of allylic hydrogen, as well as a partial oxidation mechanism consisting of acetone formation leading to combustion.

More recently, Pulido et al. used single crystal Ag(100) and Ag(111) under atmospheric conditions to study the effect of crystal facet on selectivity [15]. Based on mass spectrometry results, it was observed that PO, acrolein, acetone, and combustion products formed on Ag(100), while Ag(111) facilitated combustion only. Raman spectroscopic measurements showed that Ag(100) was more active for O_2 dissociation and oxygen atom stabilization than Ag(111). From the experimental results, combined with DFT-

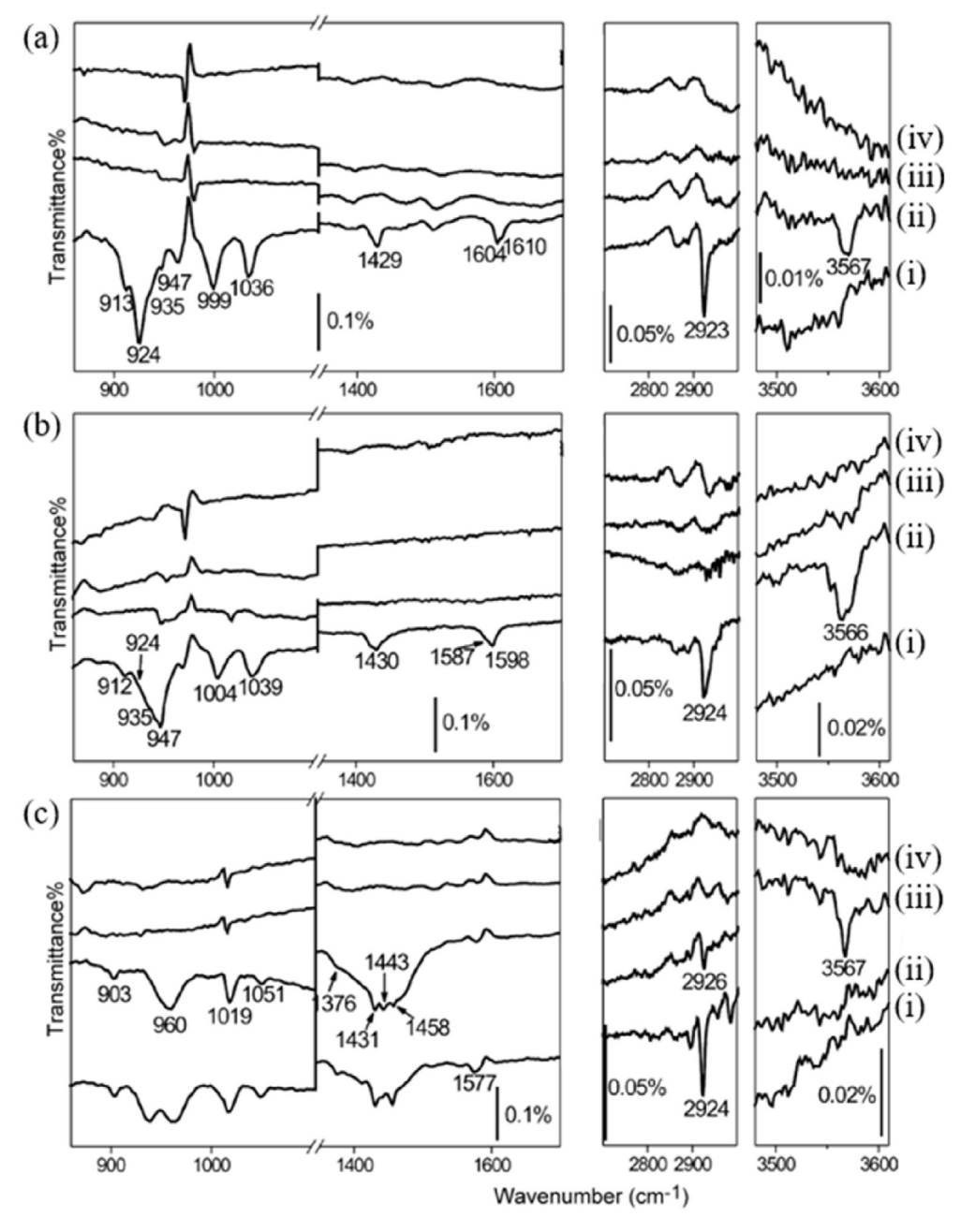


Fig. 7. RAIR spectra of 0.25 L propylene adsorbed on (a) 0.086 ML, (b) 0.291 ML, and (c) 0.5 ML oxygen-covered Ag(111) at (i) 100 K, then annealed to (ii) 200 K, (iii) 300 K, and (iv) 400 K. Reprinted with permission from Huang et al. [38]. © 2008 Elsevier B.V.

calculated activation barriers, it was suggested that both OMC formation and the allylic route were accessible on Ag(100), but only the allylic route occurred on Ag(111).

3.1.2. Using propylene oxide as a probe molecule

In addition to studying the forward reaction between propylene and oxygen, which is difficult to facilitate in UHV experiments due to the low desorption temperature of propylene, studying the adsorption and desorption of the desired product can provide mechanistic insight. Potential catalyst surfaces can be screened to determine which surfaces adsorb PO via ring opening to form the OMC intermediate and then desorb at higher temperatures as PO. TPD experiments can provide evidence of an adsorbed intermediate with increased binding energy compared to physisorbed PO, and vibrational spectroscopic measurements can be used to detect the OMC intermediate. A correlation between stabilization of this OMC and increased PO selectivity during the reaction between propylene and oxygen has been observed [20]. Using PO as a probe molecule can also provide insight into the tendency of a surface to facilitate further reaction of PO to form undesired products [61]. However, early studies with PO focused mainly on understanding the adsorption geometry and surface modification effects.

Bare studied PO adsorption on clean and oxygen modified Ag(110), and the only pathway observed was molecular desorption [48]. On clean Ag(110), PO desorbed at 179 K, with the desorption temperature increasing as a function of oxygen pre-coverage. A 30% increase in heat of adsorption was observed at an atomic oxygen coverage of 0.35 ML. The author attributed that the surface oxygen created more positively charged Ag sites, which could more readily accept electron donation from PO. This was consistent with theoretical findings from a separate study that suggested charge transfer occurred from Ag to O in an Ag–O bond, along with NEXAFS results indicating a significant ionic character of Ag–O bonds where 4d electrons of Ag donated to the 2p orbitals of adsorbed O [22].

Bare also investigated the adsorption geometry of the adsorbed PO using HREELS [48]. Overall, the vibrational spectrum was similar to that of PO in the gas phase, indicating a weakly physisorbed configuration on clean Ag(110). Based on the relatively weaker C-O-C deformation mode at 815 cm⁻¹ in the PO spectrum, the author concluded that the PO ring was not oriented perpendicular to the surface. The HREEL spectra of PO on the clean and oxygen

modified surfaces showed little difference in the observed vibrational frequencies of the normal modes due to the presence of oxygen. Ranney et al. studied PO adsorption on the Ag(110) surface modified by surface hydroxyl [46]. A smaller increase in the desorption temperature was observed with pre-adsorbed OH groups than with pre-adsorbed O, and there was no reaction between propylene and OH. Based on this, and in light of previous studies demonstrating increased epoxidation selectivity with cofed steam, the authors suggested that water vapor increased epoxidation activity by facilitating the desorption of PO [46].

While these studies provided insight into the geometry and binding energy of physisorbed PO on clean and modified Ag(110) surfaces, they did not present spectroscopic evidence of the presence of the OMC intermediate. Although the OMC intermediate has not been observed in any studies of propylene or PO on Ag-based surfaces in UHV, evidence of OMCs leading to ethylene epoxide or 1-epoxy-3-butene formation has been detected [49,64].

3.1.3. Using 1-epoxy-3-butene as a probe molecule

Another probe molecule that has been used to study the epoxidation mechanism is 1-epoxy-3-butene, an unsaturated four-carbon epoxide. Compared with PO, physisorbed 1-epoxy-3-butene desorbs from Ag surfaces at higher temperatures due to its higher molecular weight and the unsaturated C=C double bond. This suggests that it is more likely to adsorb onto the surface with sufficient energy to form a ring-opened intermediate. While 1-epoxy-3-butene is less relevant to propylene epoxidation than PO since it is the product of butadiene epoxidation, it provides a useful case study of how surface science experiments coupled with theoretical calculations can lead to development of a link between the OMC intermediate and epoxide formation. Medlin et al. observed this link on an Ag(110) model surface using TPD, HREELS, NEXAFS, and DFT calculations, showing that the adsorbed OMC leads to epoxide formation in the gas phase [49,50].

Following dosing 1-epoxy-3-butene to the Ag(110) surface at 300 K, TPD experiments showed desorption of 2,5-dihydrofuran and 1-epoxy-3-butene, indicating the presence of a strongly chemisorbed species that was not detected at lower dosing temperatures. To identify the configuration of this intermediate, HREEL spectrum of the surface following the 300 K dose was obtained, as shown in Fig. 8(a) along with DFT-calculated vibrational frequencies of the optimized OMC intermediate on a 7-atom Ag(110)

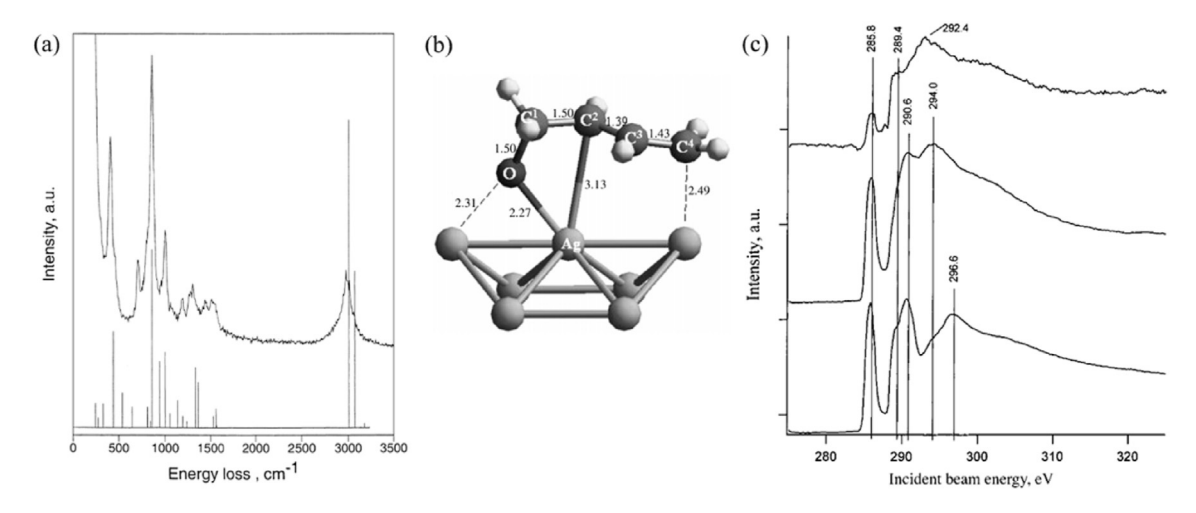


Fig. 8. (a) HREEL spectrum of 1-epoxy-3-butene adsorbed on Ag(110) surface at 300 K with vertical lines representing the calculated IR spectrum for the 1-epoxy-3-butene OMC. (b) The most stable DFT-calculated OMC intermediate. (c) C K-edge NEXAFS spectra of 20 L 1-epoxy-3-butene on Ag(110) at 120 K (lower), followed by annealing to 190 K (middle), and 50 L 1-epoxy-3-butene at 300 K (upper). (a—b) Reprinted with permission from Medlin et al. [49]. © 2000 Elsevier Science B.V. (c) Reprinted with permission from Medlin et al. [50]. © 2001 American Chemical Society.

cluster. Based on the good agreement between the experimental and theoretical vibrational spectra, especially at the most intense modes, it was concluded that the ring-opened OMC intermediate was present on the surface and underwent ring closure to form 1-epoxy-3-butene at 490 K. The binding energies of four different cyclic intermediates were calculated, and the most stable configuration, shown in Fig. 8(b), comprised a four-member ring with a single Ag atom. The relatively intense peaks at 412 cm⁻¹ and 861 cm⁻¹ corresponded to O–C–C deformation and CH₂ rocking, respectively. The authors suggested that the O–C–C deformation mode at 412 cm⁻¹ correlated with the reaction coordinate leading to ring closure of the OMC intermediate.

Further characterization of the OMC leading to 1-epoxy-3butene formation was accomplished using NEXAFS coupled with DFT calculations [50]. Displayed in Fig. 8(c), the C K-edge results showed a distinct difference between three adsorption configurations: weakly adsorbed 1-epoxy-3-butene, chemisorbed 1-epoxy-3-butene, and a ring-opened OMC intermediate. Specifically, in the spectrum of the OMC, peaks at 285.8 eV and 290.6 eV, corresponding to a π^* excited state of the C=C bond, and $\sigma^*(C^2-O)$ and $\sigma^*(C-H)$ resonances, respectively, were significantly attenuated compared to the other two more weakly bound configurations. This was consistent with the breaking of the epoxide ring and a less surface-normal configuration of the C=C bond. The attenuation of the $\pi^*(C=C)$ and $\sigma^*(C^2=0)$ resonances relative to the weakly adsorbed molecule was consistent with a suggested configuration in which binding occurred between the surface and the O in the epoxide ring. Overall, these results provided an example of how surface science experiments and DFT calculations with an epoxide probe molecule can provide a link between the OMC intermediate and the formation of the desired epoxide, along with detailed insight into the geometry of possible reaction intermediates.

We conclude this section by highlighting the gaps in direct experimental evidence of the propylene epoxidation mechanism on Ag-based surfaces. While it is often assumed that the OMC is the critical intermediate for propylene epoxidation on Ag-based surfaces, this intermediate has not yet been identified spectroscopically in UHV. Adsorbed OMC intermediates leading to the production of ethylene epoxide or 1-epoxy-3-butene have been observed and provide strong indications that the same type of intermediate is necessary for PO formation, but there exists minimal direct experimental evidence of the OMC intermediate from the reaction of either propylene or PO on Ag surfaces.

3.2. Au surfaces

Au-based supported catalysts for propylene epoxidation using H₂ and O₂ were first studied by Hayashi and Haruta in 1998 [65]. Since then, other studies have shown high PO selectivity and activity using Au/TiO₂ catalysts [66–68]. It has been necessary to cofeed molecular H₂ or water with O₂ to achieve high PO selectivity, and the most effective surface species for partial oxidation is thought to be –OOH, so the use of Au catalysts for epoxidation with molecular O₂ alone has been less well-studied. However, it is worth considering the interactions of propylene and oxygen with the Au surface and understanding the intermediates that can form. An allylic oxygen insertion pathway unique to Au-based surfaces has been identified in UHV and attributed to the presence of distinct oxygen species that are not present on Ag [11].

3.2.1. Using propylene as a reactant

Davis and Goodman [36] studied propylene TPD on clean and oxygen-covered Au(111) and Au(100) surfaces. They reported weak adsorption on the clean surfaces, as evidenced by propylene desorption peak temperatures of 150 K from Au(111) and 140 K

from Au(100). With pre-adsorbed sub-monolayer oxygen coverage, they found that propylene adsorbed more strongly with a shoulder appearing in the propylene desorption peak around 200 K. Some partial oxidation products were indicated by small 56 and 58 amu peaks at ~280 K on the Au(111) surface and a 56 amu peak on Au(100). CO₂, CO, and H₂O were also produced on the oxygen-covered surfaces.

In a later study of propylene adsorbed on oxygen-covered Au(111), Deng et al. [30] observed formation of acrolein, acrylic acid, and carbon suboxide (O—C—C—C—O). They also studied the reactions of deuterated propylene on this surface, as shown in Fig. 9 for the comparison of TPD results using different deuterated propylene molecules. They observed that when the allylic hydrogen was replaced with the less active deuterium, PO was formed. This supported the hypothesis that the easily abstracted allylic hydrogen atom was a significant cause of the much lower epoxide selectivity from propylene compared to ethylene.

Ajo et al. studied the origin of the high PO selectivity of Au/TiO₂ catalysts in UHV by depositing Au particles on a TiO2(110) surface [56]. Au was deposited using PVD, and XPS and low energy ion scattering (LEIS) were used to determine the Au island thickness and fractional coverage on the surface. Different propylene exposures were investigated, as shown in Fig. 10 for low-coverage (16%) and high-coverage (84%) surfaces. Following lower propylene exposures on both Au-covered surfaces at 120 K, a low temperature (125-155 K) and a high temperature (210-295 K) peak were observed, corresponding to desorption from the Au sites and Au–Ti interface sites, respectively. At higher exposures, a single peak with intermediate temperature (155–210 K) was observed, which was assigned to desorption from the Ti sites. The TPD peaks were assigned using LEIS peak areas recorded after annealing the propylene-covered surface to increasing temperatures. Following a low exposure (0.002 L) dose, both Au and Ti sites were masked by propylene, but after annealing the surface to ~ 225 K, the Au signal partially recovered. Then after annealing to ~380 K, both the Au and Ti signals fully recovered. The masking and recovery of the Au and Ti signal following a higher exposure (0.01 L), combined with the similar desorption temperature from clean TiO₂, confirmed the assignment of the 155–210 K peak as desorption from the Ti sites.

The authors suggested that propylene was mobile on the Aucovered TiO₂ surface, and migrated upon adsorption to the lowest energy sites at the edges of the Au islands. Using the Redhead analysis, the activation energy for desorption was shown to depend on the size of the islands, ranging from 58.2 kJ/mol on the thickest Au islands to 72.4 kJ/mol on the single-atom-thick islands. This correlation was also present for oxygen adsorption on Au/TiO₂ surfaces, and together these results helped explain the Au particle size effect that has been observed in propylene epoxidation. Overall, this study provided evidence for a synergistic effect between Au and TiO₂ where propylene binds to the edges of Au islands with higher binding energy than on Au or Ti sites alone.

More recently, Sun et al. [37] studied the reaction of propylene on an oxygen-covered Au(997) surface containing (111) terrace and step sites. In previous studies of epoxidation on model Au surfaces, the low desorption temperature of propylene from Au(100) and Au(111) surfaces caused it to desorb before it could react, so the stepped (997) surface was used in this study to allow adsorbed propylene to remain on the surface at a higher temperature (~260 K) before molecular desorption. Following propylene adsorption at 110 K and annealing to 230 K, RAIRS results revealed the C=C stretching mode at 1648 cm⁻¹ that was only detected when co-adsorbed oxygen was present, indicating enhanced propylene stability due to interactions with co-adsorbed surface oxygen. In the reaction between propylene and oxygen on the Au(997) surface, production of acrolein, CO₂, CO, and H₂O was observed. On

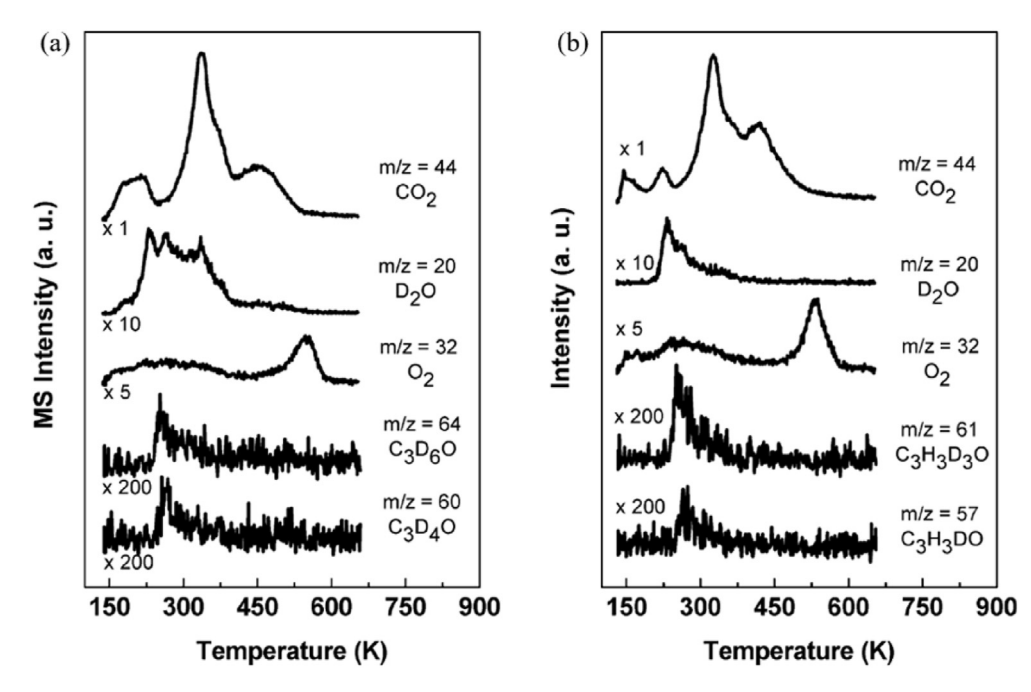


Fig. 9. TPD of two deuterated propylene molecules on O/Au(111): (a) Fully deuterated (CD₃CD=CD₂) and (b) Partially deuterated (CD₃CH=CH₂). Reprinted with permission from Deng et al. [30]. © 2006 American Chemical Society.

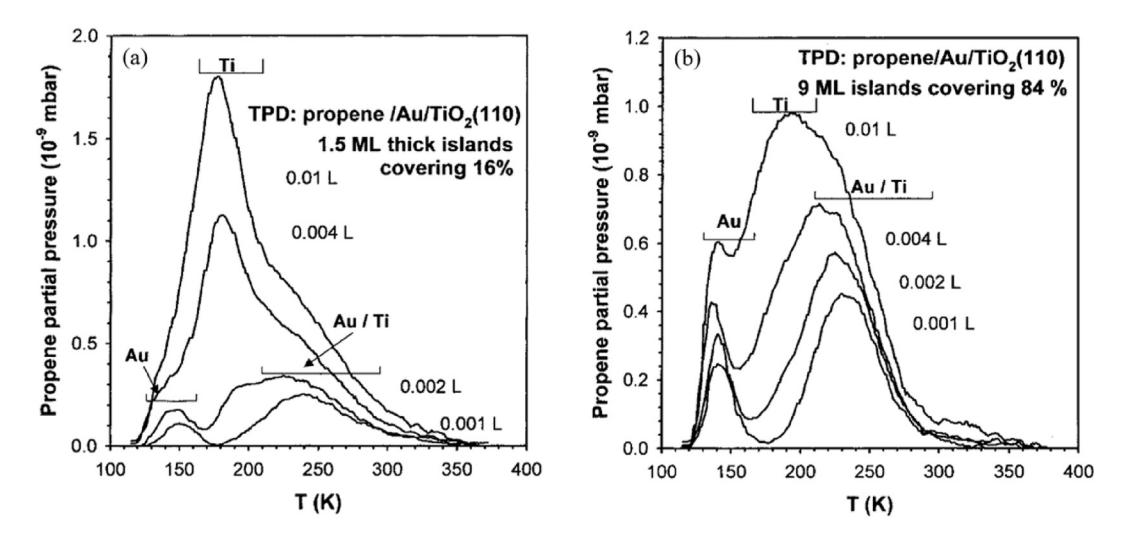


Fig. 10. TPD following different propylene exposure on (a) $TiO_2(110)$ surface 16% covered by Au islands with average thickness of 1.5 ML, and (b) $TiO_2(110)$ surface 84% covered by Au islands with average thickness of 9 ML. The corresponding adsorption sites (Au, Ti, or Au/Ti) for each peak are indicated by brackets. Reprinted with permission from Ajo et al. [56]. © 2002 Springer Nature.

the (111) step sites, partial oxidation leading to acrolein occurred at 287 K and combustion leading to CO_2 and CO occurred at 135 K. The authors concluded that molecular oxygen dissociated to form a low coverage of atomic oxygen at 287 K, facilitating the higher selectivity toward acrolein formation that was observed at higher temperatures. On the (111) terrace, molecular O_2 was the active oxygen species, and both partial oxidation and combustion occurred at 135 K. This work demonstrated dependence of propylene oxidation pathways on the nature of sites and surface species on Au.

3.2.2. Using phenylpropene as a probe molecule

Larger, aromatic molecules containing allylic H atoms have also been used as probes for their activity toward the competing reactions of partial oxidation and hydrogen abstraction. In the same way that styrene has been previously used to successfully investigate the ethylene epoxidation mechanism, different isomers of phenylpropene have been used to study propylene epoxidation. The higher desorption temperature of these aromatic compounds increased their adsorption enthalpy, leading to an increased desorption temperature compared with propylene. This allowed observation of partial oxidation pathways that were not detected when using propylene under UHV conditions. In addition, different isomers of phenylpropene forced the C=C bond into different geometries relative to the surface, providing additional routes to investigate the factors influencing epoxide selectivity.

Liu and Friend [26] used trans- β -methylstyrene as a probe molecule to study partial oxidation on Au(111) and O/Au(111). Their results were also discussed as examples in section 2.2 and 2.4.

Following adsorption at 200 K on a 0.2 ML O/Au(111) surface, they observed complete oxidation as well as three distinct partial oxidation products of trans-β-methylstyrene oxide, benzoic acid, and cinnamic acid. When 1 ML of oxygen was present prior to exposure, cinnamic acid was not formed; larger amounts of CO₂, H₂O, and benzoic acid were produced; and the epoxide desorbed in two distinct peaks. RAIRS results showed that a 1244 cm⁻¹ epoxide ring deformation mode was present following trans-β-methylstyrene oxide adsorption on clean Au(111), but not after trans-βmethylstyrene adsorption on an oxygen pre-covered surface, indicating that epoxide formation was limited by ring closing. Following heating of the oxygen pre-covered, trans-β-methylstyrene exposed surface to 320 K, the methyl (-C-H₃) stretching mode at 2918 cm⁻¹ disappeared due to oxygen insertion to form carboxylates, or proton abstraction to form decomposition intermediates. Overall, these results indicated competing pathways of allylic H and vinyl C=C bond activation, which were influenced by the oxygen pre-coverage, and they provided further evidence for the successful use of trans-β-methylstyrene as a probe molecule to study the partial oxidation of allylic olefins.

3.3. Cu surfaces

In terms of the epoxidation pathways they facilitate, Cu surfaces are more closely related to Ag than to Au. It has been shown that the oxidation state of Cu and the metal oxide structure are important factors in determining the epoxidation selectivity and the OMC intermediates on Cu-based surfaces. It should also be noted that studies using Cu-based powder catalysts have mainly focused on using O₂ alone as the oxidant (without the use of co-fed H₂ as is practiced with Au). Several previous UHV studies have presented evidence that Cu surfaces are intrinsically more selective toward partial oxidation than Ag using various probe molecules. However, only recently has spectroscopic evidence of an OMC intermediate leading to PO formation been observed, and it required the presence of a unique TiCuO_X perovskite-like surface structure to stabilize the Cu⁺ oxidation state [20].

3.3.1. Using propylene as a reactant

Many earlier studies of the partial oxidation of propylene on copper oxide surfaces focused on acrolein formation as the product of interest. Schulz and Cox used TPD to investigate propylene adsorption on the (111) and (100) surfaces of Cu₂O, and found that different desorption states were present depending on the surface structure [53]. It was also observed that propylene adsorption was sensitive to vacancies and defects in the lattice oxygen. In a different study of propylene oxidation on Cu₂O(111), Cu⁺-terminated Cu₂O(100), and O-terminated Cu₂O(100), it was found that the coordination of the surface lattice oxygen influenced selectivity toward partial oxidation products [52]. It was observed that lattice oxygen participated in the reaction, and the most selective surface toward acrolein formation was Cu₂O(111), due to the presence of coordinately unsaturated lattice oxygen. It has also been shown that the Cu₂O(111) surface was more selective toward partial oxidation than the CuO(111) surface [51]. Based on the difference in O(1s) binding energies between CuO and Cu₂O, the higher affinity toward proton abstraction and nonselective oxidation on the CuO surface was attributed to its increased Brønsted basicity. These results are consistent with the idea that interactions between Cu atoms and the active oxygen species lead to unique electronic effects that influence the selectivity of the oxidation reactions.

3.3.2. Using propylene oxide as a probe molecule

Yang et al. [20] studied the importance of the oxidation state of Cu by investigating the reactions of propylene and PO on Cu(111),

 ${\rm Cu_2O}$, and ${\rm TiCuO_X}$ surfaces. Their results were also discussed as an example in section 2.2. They used PO as a probe molecule to demonstrate the feasibility to adsorb PO as an OMC and then desorb molecularly. As shown in Fig. 11, following PO adsorption at 110 K, higher temperature shoulders were evident in the PO desorption peak on the Ti-modified surfaces (Fig. 11(c-d)) compared to ${\rm Cu}(111)$ (Fig. 11(a)) and ${\rm Cu_2O}$ (Fig. 11(b)), indicating that the Ti-modified surface had greater ability to stabilize PO. Furthermore, the Ti-modified surface had a significant PO desorption peak following the 210 K adsorption, while the ${\rm Cu}(111)$ and ${\rm Cu_2O}$ did not. These TPD results indicated that the ${\rm TiCuO_X}$ surface could stabilize an intermediate with higher binding energy than physisorbed PO, and the configuration of this intermediate was subsequently investigated using vibrational spectroscopy.

Fig. 11(f) shows the HREEL spectra following PO exposure to the TiCuO_X surface at 110 K and 210 K with DFT-calculated vibrational frequencies of adsorbed PO and OMC. Following the 210 K dose, the experimental spectrum fairly closely resembled the theoretical vibrational modes of the OMC. In addition, the strong (C-C-O) ring deformation mode that was present at 805 cm⁻¹ following the 110 K dose was significantly attenuated for the 210 K dose, and shifted to 899 cm⁻¹. The attenuation of this ring deformation mode indicated that OMC formation occurred when PO was exposed to the surface at 210 K, providing sufficient energy to overcome the barrier to ring opening. XPS provided further support for the stabilization of an OMC species on the TiCuO_X surface. Following 110 K adsorption, C(1s) XPS peaks at 285.6 and 286.8 eV (with a 1:2 ratio) were observed and assigned to the methyl and methylene carbon. respectively, indicating that the epoxide was still intact. However, after the 210 K dose, this ratio changed and the peaks shifted to slightly higher energy, suggesting the presence of a Cu-O-C carbon and an OMC intermediate.

The TPD, HREELS, and XPS results using PO as a probe molecule presented a strong indication of increased partial oxidation selectivity with the Ti-modified Cu surface. To test this activity, TPD measurements of co-adsorbed oxygen and propylene were performed on all four surfaces, and significantly higher selectivity toward PO formation was observed for the 0.6 ML $\text{TiCuO}_X/\text{Cu}(111)$ surface. This improved epoxidation selectivity of the TiCuO_X surface could be attributed to the lower basicity of the mixed-metal oxide and to the optimal oxidation state of Cu. RAIRS results using CO as a probe molecule provided evidence of a new Cu⁺ site on TiCuO_X that was not present on Cu(111) or Cu_2O . The authors concluded that the perovskite-like TiCuO_X structure stabilized the Cu^+ oxidation state and prevented its oxidation to Cu^{2+} on the surface, which was important for maintaining selective epoxidation.

3.3.3. Using phenylpropene as a probe molecule

Cropley et al. [27,55] studied trans-methylstyrene on an oxygencovered Cu(111) surface, and compared it with O/Ag(100). Epoxide formation with some decomposition was observed on oxygencovered Cu(111), while the O/Ag(100) surface facilitated only combustion with no partial oxidation. Using NEXAFS, they concluded that the adsorption geometry of trans-methylstyrene on Cu and Ag was very similar, with both the phenyl ring and the π bond being oriented parallel to the surface. This indicated that the difference in selectivity was not due to steric effects, and suggested that the Cu surface maintained a higher electrophilicity of the surface oxygen compared with the Ag surface. On Cu(111), the sequence of reactant adsorption was found to affect the types of oxygen species that were present on the surface, as discussed in more detail as an example in section 2.3. When oxygen was adsorbed after trans-methylstyrene adsorption, XP spectra showed the presence of a metastable oxygen species that was not observed when oxygen was adsorbed prior to trans-methylstyrene exposure.

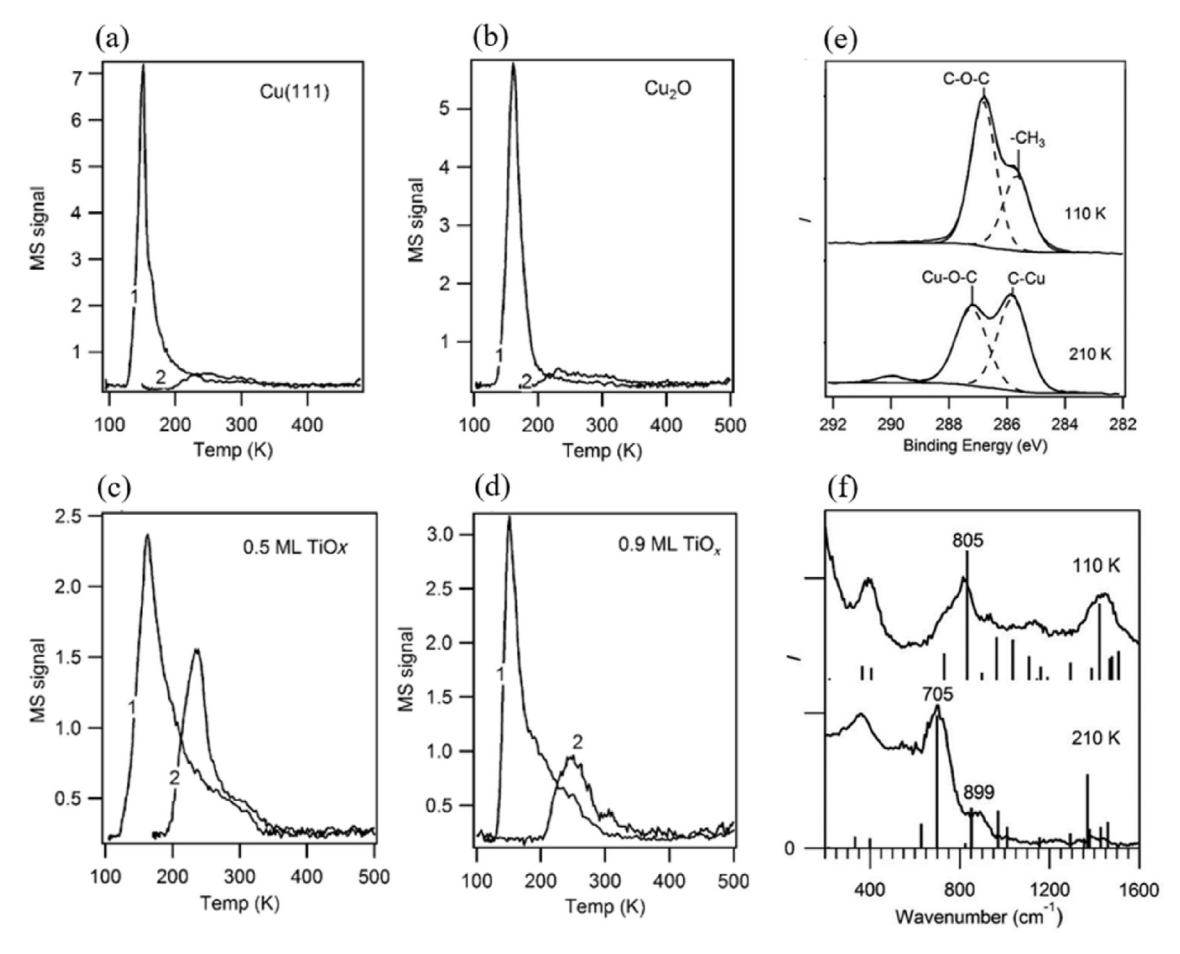


Fig. 11. TPD profiles for PO dosed at 110 and 210 K on (a) Cu(111), (b) Cu_2O , (c) 0.5 Cu_2O , (c) 0.5 Cu_2O , (d) 0.9 Cu_2O , (e) Cu_2O ,

The authors concluded that this metastable species was forced into abnormal surface sites by the presence of adsorbed transmethylstyrene. They also suggested that oxidic islands of oxygen were more readily formed when oxygen was dosed first, and these islands were not as effective for epoxidation compared with isolated atomic oxygen species.

3.3.4. Using butadiene as a probe molecule

Butadiene has also been used as a probe molecule in a study of the reaction between butadiene and oxygen on the Cu(111) surface by Cowell et al. [57]. Butadiene does not have allylic hydrogen species and so is a less useful probe molecule for studying selectivity of epoxidation versus AHS, but this study allowed investigation of the effectiveness of Cu to catalyze epoxidation as well as Cs promotion. With and without Cs, selectivity to the epoxide was 100%, but a difference in conversion due to the presence of Cs was observed. On the unpromoted surface, a maximum conversion of 50% was achieved at an oxygen coverage of ~0.05 ML, whereas with 0.07 ML of Cs the conversion approached 100%. To explain this effect, XP spectra of clean Cu₂O and several different coverages of Cs were obtained. As the Cs loading increased, a decrease of the Cu₂O peak was observed along with an increase of peaks attributed to cesium oxide, suggesting that the presence of Cs reduced the extent of oxidation of the Cu sites.

3.4. Comparison of Cu, Ag and Au surfaces

Many studies have focused on the interactions of propylene with the group IB metal surfaces by investigating the binding strength, adsorption geometry, influence of the crystal facet, and presence of oxygen. On the clean (111) surface of all three metals, a sharp propylene desorption peak below 160 K is observed, indicating that without step edges or surface oxygen species, these metals all interact weakly with propylene. It has been shown that this weakly bound propylene adsorbs with the C=C bond parallel to the plane of the surface. On oxygen-covered Ag and Au surfaces, a more strongly bound propylene configuration is indicated by a higher temperature peak, as shown in Fig. 12. Although the effect of partial oxygen coverage on propylene adsorption on Cu(111) does not appear investigated, different oxides and differently terminated structures have been shown to influence the adsorption of propylene on Cu₂O. Overall, these studies have demonstrated that when oxygen is present on the group IB metals, electron density can be transferred between surface metal atoms and oxygen species, leading to changes in the electronegativity of the adsorption site and different interactions with the π -bond of propylene or the protons of the methyl group. These electronic effects and differences in adsorption geometry can lead to differences in selectivity of the epoxidation reaction.

The reaction of propylene with pre-adsorbed oxygen has been studied in UHV on Au(111) [36], Au(100) [36], Au(997) [37], Ag(111)

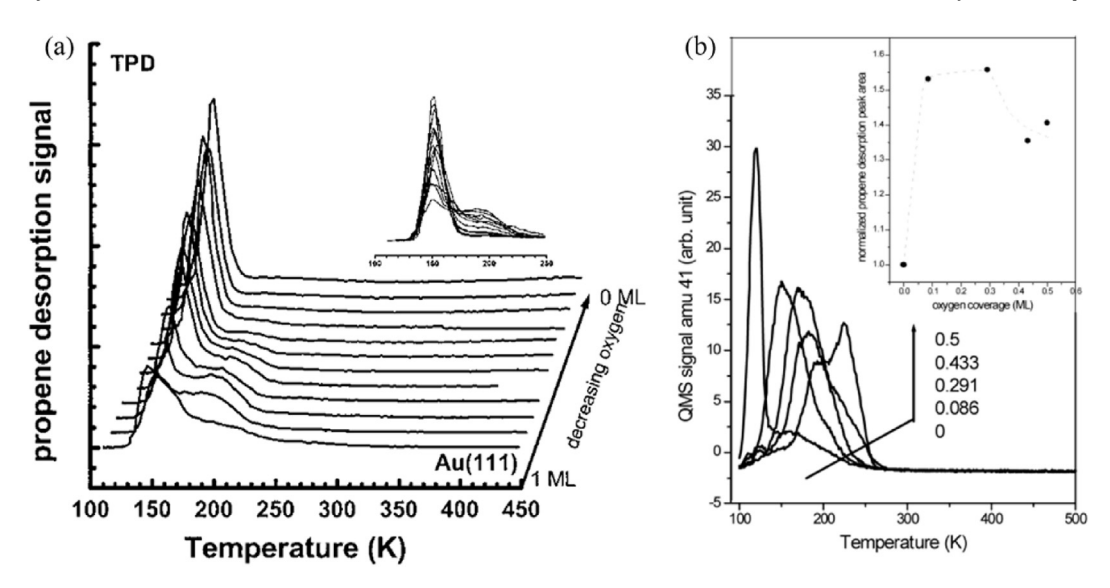


Fig. 12. TPD of propylene on (a) Au(111) with varying oxygen coverage and on (b) Ag(111) with varying oxygen coverage. (a) Reprinted with permission from Davis et al. [36]. © 2000 American Chemical Society. (b) Reprinted with permission from Huang et al. [40]. © 2002 American Chemical Society.

[38,40,41], Ag(110) [43,44,46,47], CuO [51], Cu₂O [20,51], Cu₂O(100) [52], $Cu_2O(111)$ [52], Cu(111) [20], and $TiO_X/Cu(111)$ [20]. In general, propylene either desorbs molecularly from these surfaces or reacts with oxygen to form decomposition products and, in some cases, small amounts of partial oxidation products. This slight partial oxidation selectivity has been observed on Ag(111) via acetone formation [38], on Au(111) via carbon suboxide (0=C=C=C=0), acrylic acid and acrolein formation [30], and on Cu₂O(111) via acrolein and allyl alcohol formation [52]. Most of the research on propylene oxidation on Cu oxide surfaces focused on acrolein formation as the desired partial oxidation product. Among all of these investigations of propylene oxidation in UHV, epoxide formation from propylene was only observed when using a deuterated propylene molecule on O/Au(111) [30], or propylene and O_2 on TiO_{X^-} modified Cu(111) [20]. The partial oxidation of trans-methylstyrene has also been investigated to some degree on all three metals. Combustion alone was observed on Ag(100) [55], epoxide formation was detected on Cu(111) [55], and epoxide, benzoic acid, and cinnamic acid formation was reported on Au(111) [26]. In addition, many of these studies have provided evidence that the reaction pathway of AHS led to undesirable products such as complete combustion and acrolein formation. They have also shown that the presence of different surface and lattice oxygen species influenced the interaction of propylene with the active metal sites due to electronic effects.

Another focus of these model surface studies was the spectroscopic investigation of possible reaction intermediates. All three group IB metal surfaces have shown ability to stabilize some type of OMC intermediate. An OMC intermediate leading to 1-epoxy-3-butene production has been observed on Ag surfaces, while an OMC leading to epoxidation of trans- β -methylstyrene has been detected on Cu- and Au-, but not Ag-based surfaces. Experimental evidence of an OMC leading to PO desorption has only been presented on a Cu-based TiCuO_X surface.

3.5. Plasmon-mediated catalysis

The oxidation state of the active Cu site for propylene epoxidation has also been investigated using localized surface plasmon resonance. Linic et al. [69] have shown that by illuminating plasmonic nanostructured metals with UV—vis photons, high-intensity

oscillating electric fields can be generated and lead to the formation of energetic charge carriers. The group IB metals uniquely show this photon-induced localized surface plasmon resonance. This phenomenon has been exploited to improve activity and selectivity of these plasmonic metal catalysts using illumination under more mild operating conditions than would be necessary for the normal thermal process. For example, the reaction rate of O_2 dissociation on Ag nanocubes/ α -Al₂O₃ under illumination was equivalent to the rate for the process without illumination but 40 K higher.

This effect has been used to improve propylene epoxidation selectivity by manipulating the oxidation state of Cu. Using Cu nanoparticles/SiO₂ in a packed-bed reactor, increased PO selectivity was observed under illumination compared with thermal catalysis alone [70]. The reaction rate and PO selectivity were monitored as a function of light intensity, and a threshold illumination of 550 mW/cm² was observed, above which the selectivity increased from 20 to 50% accompanied by a decrease in the reaction rate (Fig. 13(a)). To clearly compare the selectivity of the photothermal and thermal process, it was measured for several different constant reaction rates (at constant illumination of 550 mW/cm²) by varying the temperature (Fig. 13(b)). The selectivity under illumination was higher for all of the rates studied.

To investigate the underlying causes of this increased selectivity, XRD and UV-vis extinction spectra were employed. A UV-vis extinction spectrum of the catalyst after H₂ reduction displayed a distinct peak at 565 nm associated with metallic Cu, while the spectrum of the catalyst at steady state conditions (without illumination) showed a characteristic shape indicating the existence of a Cu₂O shell. Following illumination, the UV-vis spectrum dramatically changed to a spectrum closely resembling that of the post-H₂-reduction catalyst, indicating that the light induced a reduction of the oxide surface, leading to increased PO selectivity. XRD results also provided evidence for the absence of Cu₂O on the surface after the photothermal process. Overall, these results indicated that the increased selectivity for the photothermal process was due to the Cu particle surface being maintained in a reduced state during the reaction. The authors concluded that localized surface plasmon resonance of the core Cu atoms caused reduction of the oxide shell formed under reaction conditions.

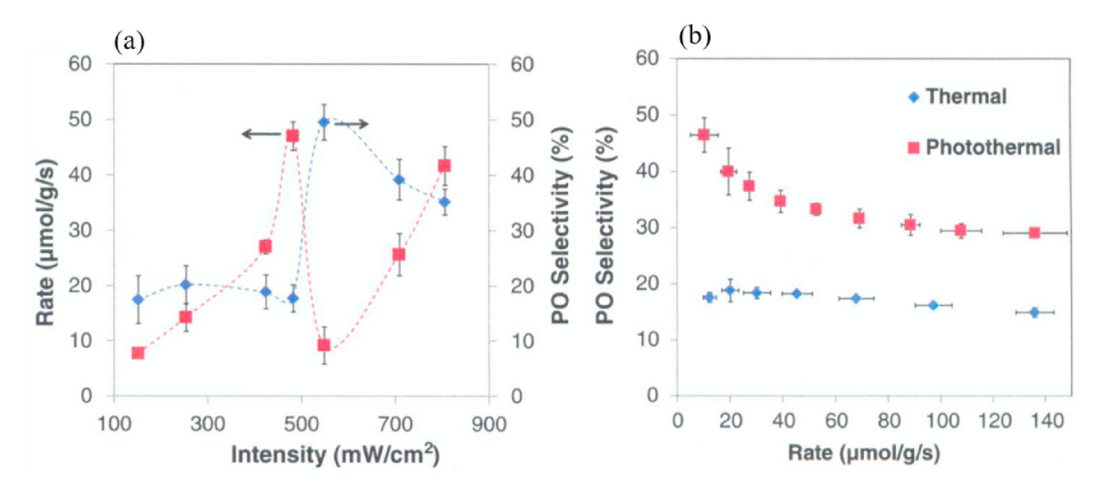


Fig. 13. (a) Propylene conversion rate (red squares) and PO selectivity (blue circles) as a function of light intensity at 473 K. (b) PO selectivity for the thermal (blue circles) and photothermal (red squares) process as a function of conversion rate. The photothermal light intensity was 550 mW/cm². Reprinted with permission from Marimuthu et al. [70]. © 2013 AAAS. (For interpretation of the references to colour in this figure legend, the reader is referred to the Web version of this article.)

3.6. Enhancing PO selectivity with shape-controlled model catalysts

One of the most significant challenges regarding research on model surfaces is the material gap between single crystal surfaces and practical supported powder catalysts. One method that has been used to bridge this gap for propylene epoxidation involves performing the reaction over powder catalysts containing shape-controlled nanocrystals with selectively exposed crystal facets. The use of these materials for epoxidation reactions was investigated by Linic et al. [71] for the production of ethylene oxide. They found higher selectivity on cubic and nanowire Ag particles, and attributed it to the selective termination by the (100) facet with under-coordinated Ag atoms. While these particles were very interesting for mechanistic understanding and displayed promising selectivity at the laboratory scale, the authors highlighted that

scaling up these materials for industrial production would require lower temperature operation, protective oxide coatings, or other methods of increased structural stability to prevent surface reconstruction to the most energetically stable configuration.

For propylene oxidation, Hua et al. [72] used capping ligands to synthesize Cu_2O nanocrystals with cubic, octahedral, and rhombic-dodecahedral shapes, selectively exposing (100), (111), and (110) facets, respectively (Fig. 14(e)). The rhombic-dodecahedra were the most selective to PO (20%), the cubic particles were the most selective for combustion (80%), and octahedral Cu_2O was most selective toward acrolein formation (60%), demonstrating control over the selectivity using particle morphology. The propylene conversion of the Cu_2O particles followed the trend octahedral > rhombic-dodecahedral > cubic. To further investigate the mechanism, surface intermediates were identified using

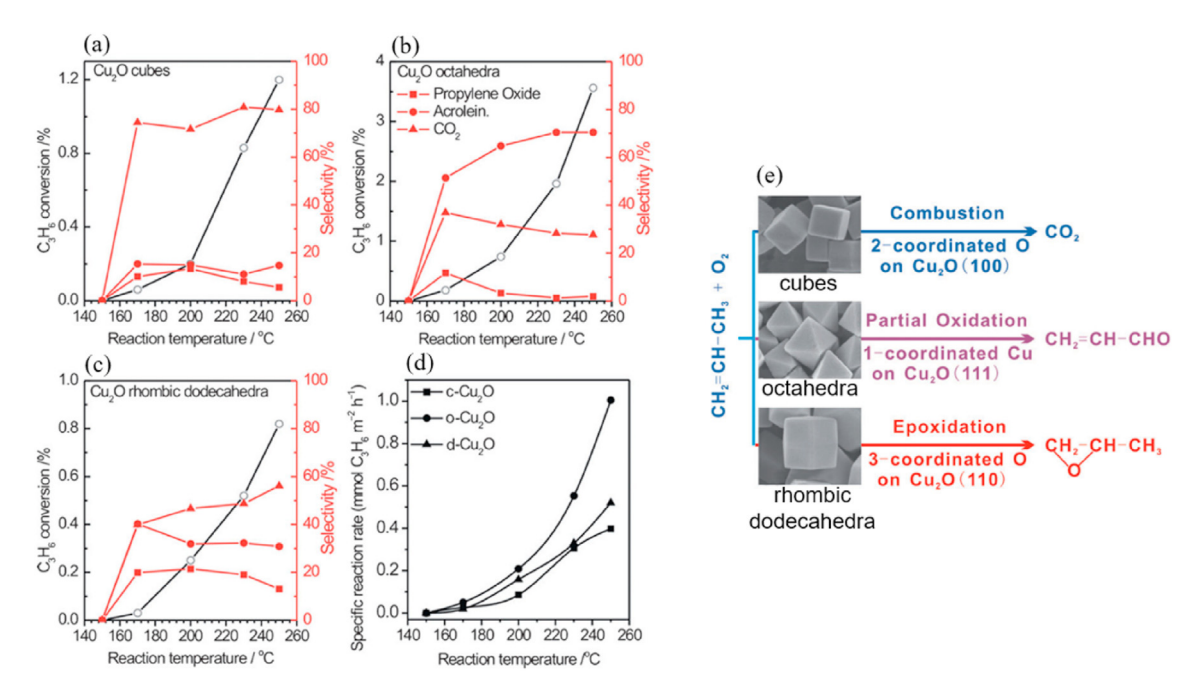


Fig. 14. Conversion of propylene and selectivity for PO, acrolein, and CO₂ vs. reaction temperature for the reaction of propylene and oxygen over (a) Cu₂O cubes, (b) Cu₂O octahedra, (c) Cu₂O rhombic-dodecahedra. (d) Specific reaction rate vs. reaction temperature for all three particle shapes. (e) Summary of experimental observations for the three particle shapes. Reprinted with permission from Hua et al. [72] © 2014 Wiley-VCH Verlag GmbH & Co.

DRIFTS. Compared with the DRIFT spectra of propylene alone, coadsorbed propylene and oxygen showed similar vibrational modes but with diminished intensities, indicating that the reaction followed a Mars-van Krevelen pathway with lattice oxygen participating rather than adsorbed oxygen. In addition, DRIFTS results combined with DFT calculations of propylene adsorption on Cu₂O(100), Cu₂O(111), and Cu₂O(110) provided evidence for unique propylene adsorption sites on the three different nanocrystal morphologies. Other chemisorbed species were also observed on the different nanocrystals: acrolein, allyl, and allene on the octahedra, CO₂ and carbonate/carboxylate on the cubic particles, and allyl and PO on the rhombic-dodecahedra. In addition, DFTcalculated activation barriers and vibrational frequencies results showed that the active sites on the cubes, octahedra, and rhombicdodecahedra were two-coordinated O on Cu₂O(100), onecoordinated Cu⁺ on Cu₂O(111), and three-coordinated O on Cu₂O(110). Overall, the results showed that the reaction selectivity could be controlled by using specific crystal facets.

Wang et al. [73] explored the effects of adding Cl^- as a promoter to cubic Cu_2O crystals with selectively exposed (100) facets. They observed a maximum of PO selectivity at intermediate Cl^- loading, indicating there existed an optimal O/Cl^- ratio for propylene epoxidation. The maximum PO selectivity of 57% was achieved with 0.33 wt% NH_4Cl , which corresponded to an equal ratio of surface Cl^- to Cu atoms. The Cl^- had a combined effect of both making the active oxygen sites more electrophilic and also occupying the active sites, which was consistent with a volcano-type correlation between selectivity and Cl^- loading.

Morphologically-controlled Ag crystal facets have also been used to study direct propylene epoxidation. Yu et al. [74] compared Ag nanocubes terminated mainly by the (100) facet to nanospheres terminated mainly by the (111) facet supported on aluminum and lanthanum oxides. For both La₂O₃ and Al₂O₃ supports, the PO selectivity on nanocubes was higher than on nanospheres, but the La₂O₃-supported nanocubes displayed the highest selectivity (51%). XRD characterization confirmed the morphology of the nanocubes and nanospheres, and XPS analysis indicated the presence of labile surface oxygen species, which were more electrophilic in nature. These results indicated that the oxide support played a significant role in the direct epoxidation mechanism through its influence on the basicity of the active oxygen site.

4. Reaction mechanism from theoretical studies on Cu, Ag and Au surfaces

DFT calculations have also played an important role in developing the mechanistic understanding of propylene epoxidation. While experimental surface science techniques are useful for identifying intermediates and proposing mechanisms, they are especially effective when combined with first principles-based theoretical calculations, which allow the determination of possible transition state geometries, activation barriers, and reaction energies. Comparing calculated energetics of different pathways helps identify the rate determining step and the reasons behind observed selectivity. For the epoxidation reaction, theoretical studies have been important for identifying the active oxygen site and simulating the surface OMC intermediate. The importance of the OMC for ethylene epoxidation is widely accepted, but for propylene epoxidation, there is continuing debate about the most selective form of the OMC and whether it is the key intermediate for epoxide formation. In the following sections, DFT studies of propylene epoxidation on the group IB metals are discussed. These are summarized in Table 2.

4.1. Ag-related surfaces

DFT studies on Ag-related surfaces have led to significant advances in understanding the active sites for epoxidation and the effects of Ag coordination and nanoparticle size. Much of the literature has focused on oxygen dissociation and the competing AHS and OMC pathways. Ideal periodic surfaces have often been studied to help understand experimental results. Kulkarni et al. [80] used DFT calculations on an Ag(111) surface to support experimental flow reactor results of PO isomerization on Ag/α-Al₂O₃, in which they observed minimal acetone, propanol, or combustion. From this it was suggested that selectivity improvements should focus on pathways from OMCs rather than further reaction of PO. Theoretically, they focused on two different OMC configurations: linear and branched, as displayed in Fig. 1. The branched OMC was 15.3 kJ/mol more stable, and led only to the formation of acetone and PO. The linear OMC had pathways to PO and several other C3 oxygenates but not acetone. The barrier to PO formation was 51.5 kJ/mol from the linear OMC and 78.4 kJ/mol from the branched OMC, suggesting that the linear intermediate was potentially more selective for epoxidation. Acrolein formation was the most thermodynamically uphill, which was consistent with an observed increase in acrolein selectivity at higher temperatures.

Molina et al. [78] performed DFT calculations on Ag_{1,83}O and Ag₂O structures atop an Ag(111) surface. Using these two surfaces allowed the study of both oxidized and non-oxidized Ag atoms on Ag_{1,83}O as well as oxidized Ag atoms on Ag₂O, as shown in the pathways in Fig. 15. Their results indicated that the presence of non-oxidized surface atoms led to a higher propylene binding energy on the Ag_{1.83}O surface compared to Ag₂O. The most stable OMC was formed on oxidized Ag atoms on the Ag_{1,83}O surface in a branched configuration (bonding to oxygen through the central carbon atom). The authors investigated various OMC intermediates on different sites and found that in general the branched arrangement was 0.15-0.20 eV lower than the linear one. On non-oxidized Ag atoms on Ag_{1.83}O, OMC formation was much more energetically unfavorable than on oxidized Ag atoms, and acrolein formation was unfeasible. This indicated that the selectivity on the partially oxidized surface was dependent on the type of active site. The energetics of the reaction pathways on Ag₂O were quite similar to those on oxidized Ag atoms on Ag_{1.83}O. In addition, the barrier to propanone formation on both surfaces was predicted to be similar to PO formation, indicating this species could also be produced from the OMC intermediate.

In an earlier paper, Molina et al. [76] studied oxygen adsorption on three different Ag surfaces along with propylene oxidation on an oxidized Ag(111) surface and nanoparticle edge sites (modeled by one-dimensional Ag rods). Pathways for PO and acrolein formation from the OMC were studied on particle surfaces and edges. They found that the barrier for acrolein formation was lower than that for PO formation on the slightly oxidized Ag(111) and Ag edge sites, as well as on the oxidized Ag edge sites. However, on the highly oxidized Ag(111) surface, the acrolein formation barrier was higher than that for PO, indicating that this surface was unique in having a higher PO selectivity. The authors attributed this difference to a unique surface oxide structure where only the subsurface oxygen was able to participate in the acrolein formation pathway with a high diffusion barrier. These results agreed with experimental observations from the same study showing the highest PO:acrolein ratio on 23.3 nm Ag particles (the largest of the three sizes studied) at 473 K, a temperature well above the reported 373 K threshold required to form subsurface oxygen on Ag. The authors also included a detailed study of oxygen adsorption on Ag surfaces for several different coverages and found the general binding energy

Table 2DFT studies related to propylene epoxidation.

Reactant	Surfaces	Model	Functional	Program	Method	Ref.
propylene, oxygen	Ag ₂ O (001)	cluster, Ag ₁₄ O ₉	B3LYP	Gaussian'03	N/A	[75]
oxygen	Ag(100), (111), (110)	7-layer slab	PBE	QuantumEspresso	N/A	[76]
propylene	O/Ag(100), (111), (110)	3-layer slab	PW91	DACAPO	Constrained	[76]
propylene, oxygen	O/Ag edge (1D rod) Ag ₂ O(001)	8-layer slab,	PW91	VASP	Minimization CI-NEB	[77]
propylene, oxygen	Ag ₂ O(001) with O vacancy	Ag ₃₂ O ₁₆ 8-layer slab,	PW91	VASP	CI-NEB	[77]
propylene	partially oxidized O/Ag(111)	Ag ₃₂ O ₁₅ 4-layer slab,	PW91	DACAPO	Constrained	[78]
propylene	fully oxidized O/Ag(111)	Ag ₁₁ O ₆ /Ag 4-layer slab,	PW91	DACAPO	Minimization Constrained	[78]
oxygen	Ag(111), (100)	Ag ₁₂ O ₆ /Ag 5-layer slab	PW91	VASP	Minimization NEB, Dimer	[79]
oxygen	Ag ₃₈ , Ag ₁₃ , Ag ₅ , Ag ₃	cluster	PW91	VASP	NEB, Dimer	[79]
propylene	Ag ₁₃ , Ag ₃ ,	cluster	PW91	VASP	NEB, Dimer	[79]
	O/Ag ₁₃ , O/Ag ₃					
propylene, oxygen	Ag(111)	4-layer slab	PW91	VASP	CI-NEB	[80]
propylene, oxygen	Ag(111), (211), (100) Au(111) Cu(111)	4-layer slab	PBE	VASP	Constrained Minimization	[81]
propylene, oxygen	Ag ₁₉ , Ag ₂₀	cluster	PW91	VASP	CI-NEB	[82]
propylene, oxygen	Ag(100), Ag(111)	5-layer slab	PW91/ B3LYP	VASP	Dimer	[15]
propylene, oxygen	Au(111) defect-free, with 1/9 ML Au adatoms,	4-layer slab	PW91	VASP	CI-NEB	[33]
	with 1/9 ML vacancies, Au(211)					
propylene, oxygen	Au(111)	4-layer slab	PW91	VASP	CI-NEB	[83]
propylene, oxygen, hydrogen	Au ₇ /TiO2	Au ₇ on 6-layer	PBE	VASP	CI-NEB	[84]
	Au ₇ /TiO2 with O-vacancy	TiO ₂ slab				
oxygen, water	Au(321)	14-layer slab	PBE	VASP	Dimer	[85]
oxygen, hydrogen	Au(321)	14-layer slab	PBE	VASP	Dimer	[85]
propylene	O/Au(321)	14-layer slab	PBE	VASP	Dimer	[85]
propylene	OOH/Au(321)	14-layer slab	PBE	VASP	Dimer	[85]
propylene	OH/Au ₇ /Al ₂ O ₃	Au on oxide slab	PW91	N/A	Constrained	[86]
propylene	1D Au _{rod} /TiO ₂ Cu ₂ O(111) O ⁻ /Cu ₂ O(111)	12-layer slab	PBE	VASP	Minimization CI-NEB	[34]
	$O_2^-/Cu_2O(111)$					
propylene, oxygen	Cu(111) Ru–Cu(111)	4-layer slab	PW91	VASP	CI-NEB	[87]
propylene, allyl, C ₃ H ₅ O, acrolein, OMC, PO, propanal acetone		9-layer slab	PBE	VASP	NEB	[88]
propylene, oxygen	Cu(111)	4-layer slab	PW91	VASP	CI-NEB	[89]
propylene, SO ₂	Ag(111) Cu ₂ O(001)	4-layer slab	PW91	VASP	CI-NEB	[32]
propulano	CuO(001)	12 layer dab	PBE	VASP	CI-NEB	[00]
propylene propylene	Cu ₂ O(111) Cu ₂ O(110)	12-layer slab 6-layer slab	PBE	VASP	CI-NEB	[90] [90]
OMC containing transition metal dimer in vacuum	N/A	cluster	VWN	ADF	N/A	[91]
propylene	RuO ₂ (110) O/RuO ₂ (110)	9-layer slab	PW91	VASP	CI-NEB	[92]
propylene, oxygen, water	Au ₃₈ cluster Au ₁₀ cluster	cluster	PBE	DMol	LST/QST	[93]
propylene, oxygen	FeH ₁₉ O ₇ Si ₇	cluster	B3LYP	Gaussian09	N/A	[94]
hydrogen, oxygen	Au ₃	cluster	BPW91	Gaussian98	STQN	[95]
propylene, oxygen, hydrogen	Au ₃	cluster	B3LYP	Gaussian03	Constrained Minimization	[95]
water, peroxide, ethene, ethylene epoxide	Ti[-O-Si(OH) ₃] ₄	cluster	BP	DMol	EF	[96]
propylene	H ₂ O ₂ /TS-1	cluster	BPW91	Gaussian98	Constrained Minimization	[97]
propylene, peroxide	$TiSi_{15}O_{20}H_{28}$	cluster	B3LYP	Gaussian09	Berny	[98]
propylene, peroxide	TiSi ₁₄ O ₁₉ H ₃₀	cluster	B3LYP	Gaussian09	Berny	[98]
propylene, peroxide	TS-1	cluster	BPW91	Gaussian98	STQN	[99]
peroxide	Ti(OH) ₄	cluster	B3LYP	Gaussian98	N/A	[100]
ethylene	Ti(OH) ₃ (OOH)	cluster	B3LYP	Gaussian98	N/A	[101]
propylene, peroxyformic acid	N/A	N/A	B3LYP	Gaussian94	ACES	[102]
propylene, dioxyrane	N/A	N/A	B3LYP	Gaussian94	ACES	[102]
propylene, dimethyldioxyrane	N/A	N/A	B3LYP	Gaussian94	ACES	[102]
propylene, dioxyrane	N/A	N/A	B3LYP	Gaussian94	N/A	[103]
propylene, dimethyldioxirane	N/A	N/A	B3LYP	Gaussian94	N/A	[103]

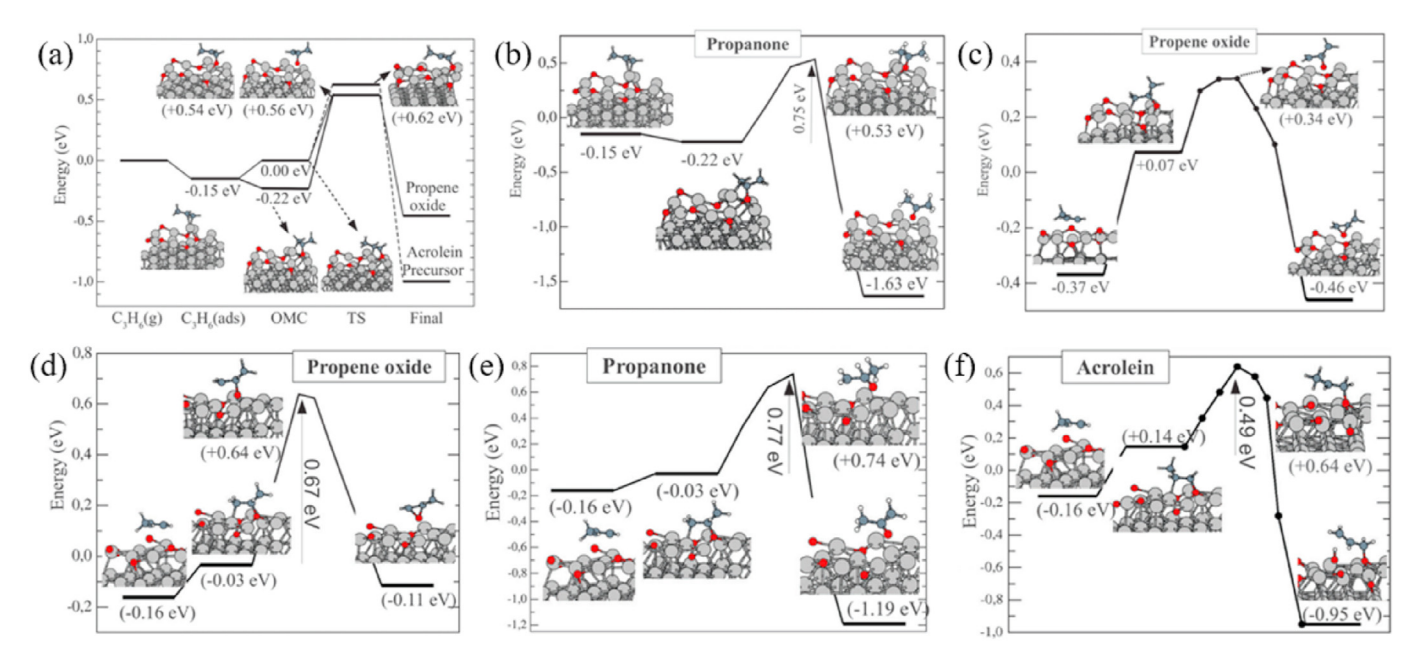


Fig. 15. (a) Reaction pathways for acrolein or PO formation from propylene adsorbed on oxidized Ag atoms on the $Ag_{1.83}O$ surface. (b) Propanone formation on oxidized Ag atoms on $Ag_{1.83}O$. (c) PO formation on non-oxidized Ag atoms the $Ag_{1.83}O$ surface. Pathways for (d) PO, (e) propanone, (f) acrolein formation on the $Ag_{2}O$ surface. Reprinted with permission from Molina et al. [78]. © 2014 Royal Society of Chemistry.

trend to follow (100) > (110) > (111). Using calculated surface energies and Wulff constructions for supported silver particles, they found that the (100) to (111) facet ratio increased with oxygen partial pressure.

Pulido et al. [15] identified detailed OMC and AHS reaction pathways on Ag(100) and Ag(111) surfaces, and concluded that the rate-determining step was the dissociation of the O₂ molecule. Different adsorption configurations of propylene relative to the surface oxygen led to different pathways. Their results confirmed that hydrogen abstraction leading to combustion was the most kinetically favored pathway on silver. By comparing the activation barriers for epoxidation via the OMC, the authors found that partial oxidation was possible on Ag(100), but inaccessible on Ag(111). This agreed with mass spectrometry results (previously discussed in section 3.1.1) showing selectivity toward to PO, acetone, acrolein, and CO₂ formation on Ag(100), but only CO₂ production on Ag(111).

Fellah et al. [75] used an $Ag_{14}O_9$ cluster to represent the $Ag_2O(001)$ surface and found that PO and π -allyl formation had similar reaction barriers, which was not the case on the Ag(111) surface. They attributed this to subsurface oxygen and lower Lewis basicity of surface oxygen species on the silver oxide compared to O/Ag(111), which was confirmed by a comparison of SO_2 binding energy on these surfaces. The mechanism on the $Ag_2O(001)$ surface was also studied by Tezsevin et al. [77] using a periodic calculation. Interestingly, they found that PO formed readily on the surface, but was not favored as a product due to its high desorption energy. Additionally, AHS of PO had a 1.4 eV lower barrier than the AHS of propylene, suggesting that direct allyl formation was not favorable, but allyl formation still occurred through a PO intermediate.

Cluster calculations have also been used to investigate propylene epoxidation mechanisms on nanoparticles (NP) and subnanometer particles. Cheng et al. [82] studied Ag_{19} and Ag_{20} clusters in vacuum and on the amorphous alumina support to determine the effects of spin, active site, and support on oxygen dissociation and propylene epoxidation. It was found that spin state had little effect on the reaction, but the nature of the active site

influenced both O2 dissociation and epoxide selectivity. O2 dissociation was more favorable at interface sites than those on top of the cluster, and oxygen atoms on the Ag side of the interface were more active for epoxidation than those on the support side. This theoretical prediction of higher activity due to the particle-support interface agreed with propylene oxidation experiments from the same study on nanocrystalline diamond-supported Ag clusters, which displayed no activity, in contrast to Ag clusters of similar size on alumina. Boronat et al. [79] compared energetics of O2 dissociation on cuboctahedral clusters of Ag₃₈ and Ag₁₃, planar clusters of Ag₅ and Ag₃, as well as Ag(111) and (100) periodic surfaces. The larger particles and periodic surfaces had lower barriers for O₂ dissociation, and a relation was observed between the activation barrier and the coordination number of Ag atoms involved in the transition state. They also studied the reaction of propylene with adsorbed O, O2, and OOH on Ag3 and Ag13 clusters and found that on some surfaces the OMC could not form, and AHS was favored on every surface studied. The authors supported the DFT result experimentally by showing that CO₂ formation was favored in the reaction of propylene and oxygen on zeolite-supported Ag₃ and TiO₂-supported Ag₁₅₋₂₀ clusters.

The results from these DFT studies were consistent with the experimental trends that have been observed on Ag model surfaces and catalysts. The theoretical results on Ag cluster reshaping and surface crystallinity by Molina et al. [76] were consistent with Ag particle morphologies observed under vacuum and reaction conditions using HRETEM and GISAXS. In addition, the authors utilized DFT-calculated reaction barriers to develop mechanistic reasoning for experimentally observed particle size-dependent selectivity. Pulido et al. [15] coupled their theoretical results with experimentally observed selectivity on Ag(111) and Ag(100) surfaces. DFT studies of Ag clusters have connected theoretical conclusions about interfacial effects to experimental studies of the epoxidation reaction on catalysts containing different sizes of Ag particles on various supports [82].

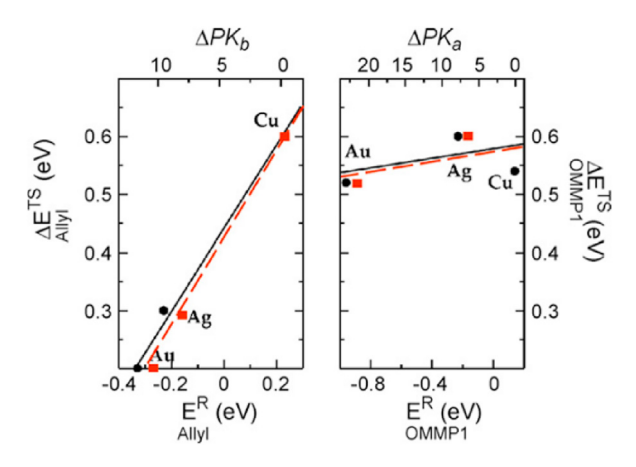


Fig. 16. Activation barriers versus reaction energies plotted for allyl and branched OMC (OMMP1) intermediate formation on Cu, Ag, and Au surfaces. Reaction energy has also been converted to PK scale on a separate axis. Reprinted with permission from Roldan et al. [83]. © 2009 Elsevier B.V.

4.2. Au-related surfaces

Propylene epoxidation using Au-based catalysts has been shown to follow unique pathways not observed on Cu or Ag surfaces. Roldan et al. [83] studied the adsorption of propylene on Au(111) and the reaction of propylene with oxygen-covered Au(111) to form an OMC intermediate or undergo dehydrogenation. They found that formation of the branched intermediate had 0.26 eV higher activation barrier than the linear OMC (called OMMP1 in Fig. 16), suggesting that propylene and oxygen would not readily form the branched intermediate. The results revealed that the barrier for allyl intermediate production was 0.32 eV lower than that for linear OMC formation, consistent with the experimentally observed low PO selectivity on oxygen modified Au surfaces. Combining with previous studies on Cu(111) and Ag(111) surfaces, a correlation between the activation barrier and the reaction energy for the formation of both the allyl and the OMC intermediate followed the Brönsted-Evans-Polanyi (BEP) relationship (Fig. 16). They also estimated acid-base constants from the reaction energy and revealed that the selectivity was dependent on the basicity of the adsorbed oxygen.

Baker et al. [33] found an opposite barrier difference between the two types of OMCs on Au(111), with the formation of the branched intermediate being slightly favored over the linear configuration. They also investigated the influence of various defects. Of the two pathways investigated, the AHS barrier was lower than that for OMC formation on both the defect-free surface and Au(111) with 1/9 ML of vacancies. On the stepped surface, Au(211), the barrier for AHS was more than twice that on the defect-free surface, and the authors correlated this with the energy associated with oxygen deformation necessary to abstract the hydrogen atom. The authors also calculated the Bader charge of oxygen adsorbed on the four different surfaces to try to explain the AHS barrier difference, but the estimated charge did not vary significantly between the surfaces. Propylene adsorption energy followed the trend: defect-free < vacancy < step < adatom, which they explained by an increase in electron density localization when Au adatoms were present.

Moskaleva [85] compared propylene epoxidation pathways when O and OOH species were used as the oxidant on the Au(321) surface. In addition to looking at branched and linear configurations, they also consider five-membered OMC intermediates involving two Au atoms and four-membered intermediates

involving one Au atom. Although the five-membered ring was more thermodynamically favorable, the four-membered one had a lower barrier to epoxide formation. With atomic oxygen as the oxidant, formation of the branched intermediate was calculated to have a lower barrier than the linear configuration. They found that the five-member OMC needed to pass through a four-member ring in order to form the epoxide, and that the formation of propanal and acetone had lower barriers than PO. This was consistent with low selectivity on Au catalysts using molecular O₂. With OOH as the oxidant, pathways with higher selectivity for epoxide formation were identified due to high barriers of competing reactions such as acetone formation and AHS.

The influence of the TiO₂ support was investigated by Zhang et al. [84] using a Au_7 cluster on top of a $TiO_2(001)$ surface. They found that the most stable adsorption configuration of the cluster was one in which the Au cluster donated charge to titania. Adsorption of O₂ and C₃H₆ were most stable away from the interface, on the Au atoms on top of the cluster. With defect-free titania, the reaction leading to PO formation went through a two-metal OMC intermediate and took place on top of the cluster. No side products were considered. With H₂ present, the overall epoxide formation reaction was more exothermic and the OMC was bonded to a single Au atom. They also studied the reaction with an oxygen vacancy in the titania next to the Au₇ cluster, which made the total charge on Au₇ negative rather than positive. The O₂ on top of the cluster was more readily activated in this case, but the lowest energy adsorption site was at the vacancy. The epoxidation pathway with on-top Au atoms was similar to the defect-free surface, but was slightly more thermodynamically favorable. When O2 was adsorbed at the interface, the reaction was much more thermodynamically favorable due to the ability of the O atom to fill the vacancy upon O-O bond cleavage and PO desorption. O2 dissociation at the vacancy had a low barrier, but the negative charge made OMC formation kinetically unfavorable. With OOH at the interface as the oxidant, the barrier for OMC formation was lower than all other pathways studied. From these results, they concluded that the OOH species was the most selective oxidant for epoxidation on this surface, and oxygen vacancies were also important.

While TiO₂ has generally been accepted as the best support for epoxidation with Au, Lee et al. [86] compared Au/TiO₂ with Au₇/ Al₂O₃ and found indications of higher activity using alumina as the support. Their calculations showed that peroxo radicals were necessary to form the OMC on TiO2 supported Au, but the OMC could form immediately following adsorption of propylene on Al₂O₃ supported Au. They found that on both surfaces, the ring closing step had the highest activation barrier, and left behind an oxygen vacancy that had to be filled via oxygen adsorption, for which dissociated hydrogen was necessary on TiO2, but not on Al₂O₃. To provide experimental evidence of the activity of Al₂O₃ supported Au catalysts, the authors studied the propylene oxidation reaction on a thin film of sub-nanometer Au clusters on Al₂O₃ prepared by atomic layer deposition. They found high activity for all three gas mixtures studied (propylene $+ O_2$, propylene $+ O_2 + H_2$, and propylene + O₂ + H₂O), and, notably, an especially high PO:acrolein ratio was observed when water was included in the reaction mixture. This indicated that on Al₂O₃ supported catalysts, co-fed water could replace the hydrogen that is commonly used for propylene epoxidation with TiO₂ supports. This result also agreed with the theoretical finding that surface peroxo radicals were not needed to form the OMC on Au₇/Al₂O₃, in contrast with Au/TiO₂.

Overall, these theoretical studies of propylene epoxidation on Au surfaces provided mechanistic insight into experimental results on Au-based catalysts. First, they revealed that in the epoxidation of propylene on oxygen modified surfaces, Au showed an intrinsically lower activation barrier to AHS than Cu or Ag, consistent with

experimental results showing the necessity of co-fed hydrogen or water for increased PO selectivity. In addition, DFT studies revealed that these co-reactants provided sources of surface hydroxy or peroxo species that could reduce the activation barriers of certain steps in the epoxidation mechanism.

4.3. Cu-related surfaces

Cu has increased ability over Ag and Au to stabilize oxygen, which causes it to form oxide structures under reaction conditions when oxygen is present. It has been shown to be more selective than Ag and Au due to less basic oxygen species participating in the epoxidation reaction [81]. For these reasons, theoretical studies of Cu have mainly focused on probing the mechanism and oxidation state using Cu oxide surfaces rather than metallic Cu.

Düzenli et al. [32] provided insight into the differences between $\text{Cu}_2\text{O}(001)$ and CuO(001) surfaces for epoxidation. Their results were also discussed as an example in section 2.5. They found that on the CuO surface, the cyclic intermediate was a bridge between two oxygen atoms rather than one oxygen and one Cu. The formation of propylene oxide from this intermediate had a barrier of 2.90 eV compared to the barrierless formation of acrolein from the allylic intermediate, indicating that the CuO surface was selective toward acrolein. On the other hand, the Cu2O surface stabilized a branched OMC intermediate and an allylic intermediate. The allylic intermediate was more stable by 1.56 eV, and the barrier for the formation of PO from the OMC was slightly lower than that toward acrolein formation from the allylic intermediate. Their results of more facile acrolein formation on CuO supported the importance of low surface oxygen basicity for enhanced PO selectivity.

Song et al. [88] performed further studies into the CuO surface by investigating the differences between propylene epoxidation on the (111) and (100) facets. They found similar adsorption energies between the two different propylene OMC intermediates on both the (111) and (100) facets. On CuO(111), the formation of acrolein was more exothermic and kinetically favored. The (100) facet had pathways leading to the formation of PO, acetone, and propanal. They found that the d-orbitals of Cu in CuO(100) were closer to the Fermi level than those in CuO(111) due to under-coordinated Cu atoms.

In a subsequent study, Song et al. [34] compared the lattice, atomic, and molecular oxygen pathways on a $Cu_2O(111)$ surface (Fig. 17) and found that while atomic oxygen was the most active, surface O_2^- was the most selective for PO formation, and they explained this by its low basicity relative to atomic oxygen. They used hydrogen binding energy as a probe for the basic character of

the oxygen species, finding that the binding energy with atomic oxygen was 0.80 eV lower than with surface O_2^- , consistent with the calculated barriers for the AHS pathway. Although surface O_2^- had the smallest energy difference between the epoxidation and dehydration barriers, AHS was still the more favorable pathway. They investigated this further by comparing C—H bond scission and C—O bond formation. Projected crystal orbital Hamilton population diagrams for the transition states of these two reactions revealed a larger population of bonding states for the C—H bond breaking TS, indicating higher stability of the TS for the C—H bond breaking pathway.

Theoretical studies of propylene epoxidation on Cu have provided useful insights into experimental trends on Cu model surfaces, especially regarding the high acrolein selectivity that has generally been observed on oxides of Cu. DFT calculations have shown that the oxygen basicity was an important factor in determining if this undesirable AHS pathway would occur. In addition, DFT studies have improved the understanding of how surface structure and oxygen species influenced selectivity, providing useful information for the development of surfaces with stabilized Cu oxidation state and surface oxygen species to increase PO selectivity.

4.4. Comparison of Cu, Ag and Au surfaces

Torres et al. [89] compared theoretical results of propylene epoxidation on both Cu(111) and Ag(111), and found that formation of the allylic intermediate was kinetically favored on O/Ag(111), while OMC formation was favored on O/Cu(111). The main difference between the energy barriers on the two surfaces was present in the formation of intermediates, which was significantly influenced by the orientation of the adsorbed propylene. Fig. 18(a) displays four possible orientations of the propylene relative to oxygen adsorbed on the hollow site. The proximity of the allylic hydrogen and the vinyl hydrogen to the oxygen adatom influenced the selectivity. The reaction profiles for the formation of the intermediate and product are displayed in Fig. 18(b-c), where the Cu and Ag surfaces kinetically favored AHS by 0.30 eV and 0.06 eV, respectively. Combined with the profile for the further reaction of the products, this led to a predicted 99% combustion selectivity on the Ag surface and 50% PO selectivity on Cu. This difference was explained by the basicity of the active sites. Using a SO₂ probe molecule, they reported much lower Lewis basicity for the oxygencovered Cu surface, further supporting the hypothesis that the control of surface oxygen basicity was an important design criterion.

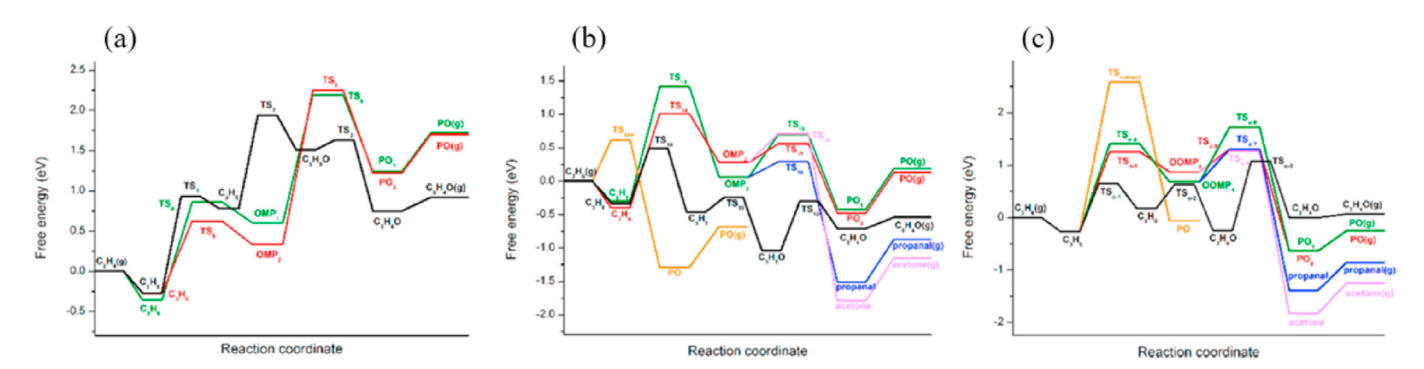


Fig. 17. Pathways of propylene epoxidation on $Cu_2O(111)$ with different oxidants: (a) O^{2-} (b) O^{-} (c) $O_{\overline{2}}$. Green and red lines show PO formation from the linear (OMP1) and branched (OMP2) OMC, orange lines show direct PO formation, black lines show acrolein formation, blue lines show propanal formation, and pink lines show acetone formation. Reprinted with permission from Song et al. [34]. © 2018 American Chemical Society. (For interpretation of the references to colour in this figure legend, the reader is referred to the Web version of this article.)

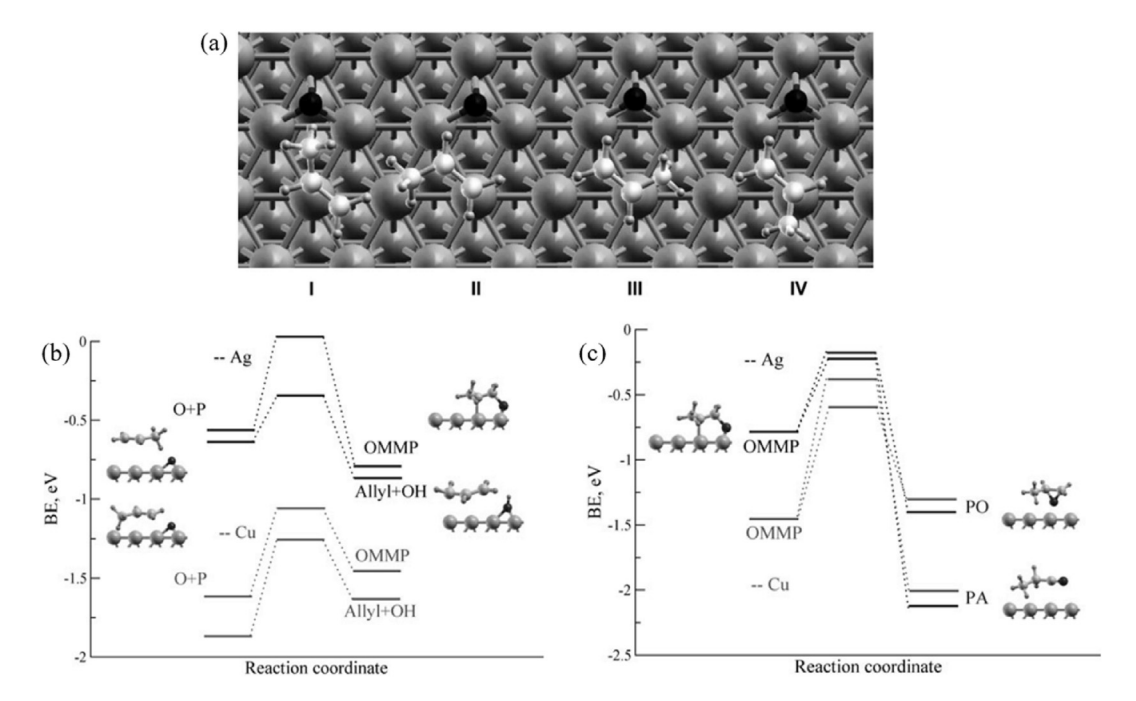


Fig. 18. (a) Configurations of adsorbed propylene and oxygen on periodic surface. (b) Comparison of pathways toward OMC and allylic intermediates on Ag(111) and Cu(111) surfaces. (c) Calculated reaction profiles for PO and aldehyde formation from OMC intermediate. Reprinted with permission from Torres et al. [89]. © 2007 Wiley-VCH Verlag GmbH & Co. KGaA.

Taken together, these studies point to the importance of metal surface electronegativity and electronic properties of the participating oxygen species for achieving high PO selectivity. Differences in selectivity on Cu and Ag surfaces have been attributed to the Lewis basicity of the oxygen species, and theoretical studies have shown that molecular oxygen is the most selective oxidant on these surfaces, although both Cu and Ag surfaces facilitate O2 dissociation. On Au surfaces, the highest selectivity is observed when the oxidant is a peroxide species [85]. For pathways toward the formation of the allyl and OMC intermediates on Cu, Ag, and Au, the correlation between the calculated activation energy and reaction energy follows the BEP relationship [83]. In addition, by using cluster calculations and comparing different crystal facets and oxide structures, DFT studies have shown that the coordination environment of the active metal atom is also influential in propylene epoxidation selectivity. Overall, many of the observed experimental results on model surfaces can be better understood with the additional insight gained from these theoretical studies. More detailed, surface-specific mechanisms can be proposed, and differences in selectivity can be more clearly attributed to certain defects, active oxygen species, or metal oxide supports, among others.

5. Studies on other model surfaces

5.1. Experimental studies on other surfaces

While Cu, Ag, and Au surfaces have been studied extensively, there have also been surface science studies of the propylene epoxidation reaction on surfaces other than the group IB metals, offering further insight into the factors affecting PO selectivity. In a study of both isobutene and propylene oxidation on $TiO_2(110)$, Robbins and Henderson mainly reported results for isobutene, but they included preliminary work with propylene oxidation [58]. Following propylene adsorption on clean $TiO_2(110)$ at 95 K, only molecular desorption of propylene was observed at approximately

160 K. On oxygen pre-covered $TiO_2(110)$, they observed partial oxidation of propylene in the form of acetone and propanal formation.

Due to their high oxidation activity, Pt-based catalysts have been studied for deep oxidation of propylene rather than partial oxidation. On clean Pt(111), propylene interacted relatively strongly with the surface in a di- σ -bonded configuration [61]. When oxygen was present on the surface, complete oxidation occurred, and the product distribution was dependent on the oxygen pre-coverage. Propylene adsorbed on Pt(111) with excess oxygen resulted in the formation of CO2 and water, while propylene with lean oxygen coverage resulted in both reforming and combustion products. Two major steps of the complete oxidation pathway were identified on Pt(111): oxidative dehydrogenation of the vinyl proton with desorption of water, followed by skeletal oxidation of the dehydrogenated propylene above 300 K. Interestingly, when propylene with a deuterated methyl group was used, the initial water desorption peak at 285 K was entirely H₂O, while HDO and D₂O did not desorb until near 365 K. This indicated that complete oxidation on Pt was initiated by the abstraction of the vinyl proton, while the allylic proton remained intact. Only complete oxidation was observed except at very high propylene coverages, when acetone and acetic acid were formed as well. Isotope labeling studies suggested that the methyl protons were not removed in the formation of partial oxidation products and again provided evidence that the vinyl proton was less stable on the Pt(111) surface. This more facile activation of the vinyl proton on the O/Pt(111) surface was in contrast with the mechanism that has been proposed with Cu-, Ag-, and Au-based catalysts, in which dehydrogenation of the allylic proton appeared to initiate complete oxidation.

The propylene oxidation reaction on Rh has also been studied in UHV with a focus on understanding the hydrogen activations that lead to different pathways. On Rh(111), propylene reacted with preadsorbed oxygen to form acetone, CO₂, CO, and H₂O [60]. Molecular desorption and complete oxidation were observed at all oxygen coverages, while the formation of acetone only occurred at oxygen

coverage above 0.45 ML, indicating that oxygen could inhibit C—H bond activation. Isotopic labeling experiments showed that the partial oxidation pathway leading to acetone involved breaking the C—H bond on the central C atom of propylene, and no allylic H atoms were involved. Overall, these results indicated that oxygen interacted with Rh metal in a dramatically different way than group IB metals.

5.2. Theoretical studies on other surfaces

The propylene epoxidation mechanism on MoO_X/SiO_2 was recently investigated by Wan et al. using DFT [104]. On MoO_X/SiO_2 , the active oxygen species was a four-fold coordinated surface Mo=0 complex, and the barrier to PO formation from the OMC was found to be nearly double that for both AHS and acrolein formation from the allylic intermediate, suggesting a low PO selectivity via the typical OMC pathway on the MoO_X surface. The authors also investigated the interaction of gas phase radicals (formed from AHS) with adsorbed O_2 and propylene, and found that the reaction between $C_3H_5OO^*$ and propylene led to PO formation with a lower barrier than propanal and acetone. They suggested that while the gas phase $C_3H_5OO^*$ is an effective oxidant, the $C_3H_5O^*$ that formed from its reaction with propylene mainly facilitated dehydrogenation, thereby limiting the PO selectivity in this free radical pathway.

Propylene epoxidation with both lattice oxygen and surface adsorbed oxygen was studied theoretically on RuO₂(110) surfaces [92]. The activation barrier to formation of the branched OMC. which was the more stable and accessible intermediate, was 0.19 eV with lattice oxygen (on stoichiometric RuO₂) and 0.05 eV with ontop adsorbed oxygen (on oxygen-covered RuO2), which was consistent with the more weakly bound, electrophilic nature of the latter oxygen species. Epoxidation using this species had lower activation barriers to PO formation from both OMC intermediates, indicating that the oxygen-covered surface would be more selective to epoxidation. This was further supported by the highly stabilized OMC species on stoichiometric RuO₂, which had lower barriers to decomposition than epoxidation. In addition, the stoichiometric surface had a higher barrier for the direct oxygen insertion route, where PO was formed directly from adsorbed propylene rather than through a surface OMC intermediate. On the oxygen-covered surface, this direct pathway was exothermic. Overall, the authors concluded that the stoichiometric RuO₂(110) surface with lattice oxygen facilitating epoxidation would not show strong performance for PO formation when compared with the surface covered with adsorbed oxygen.

6. Conclusions and future opportunities

In this review, experimental and theoretical surface science investigations of direct propylene epoxidation using molecular oxvgen have been discussed. The group IB metals are the most promising surfaces for this reaction primarily due to their ability to stabilize surface oxygen for partial oxidation. Through experimental and theoretical studies on model surfaces, an understanding of the active sites on these metal surfaces and the mechanism of propylene epoxidation has been established. The results summarized here have demonstrated the impact of the basicity of the oxygen sites and the electronic characteristics of the active sites on selectivity. For example, DFT studies on Ag(111) and Cu(111) showed the influence of surface oxygen sites on AHS and adsorbed propylene orientation; UHV experiments used a Ti-modified Cu oxide surface to control the oxygen basicity, stabilize the OMC intermediate, and improve PO selectivity. These two examples demonstrate how fundamental understanding can lead to improvements in catalyst design, but they also highlight the

difficulties in controlling the electronic properties and adsorbate orientations to enhance PO selectivity.

In particular, the unique interaction of oxygen with the group IB metals underlies important mechanistic principles regarding the design of effective catalysts for propylene epoxidation. These principles can be summarized as follows: (1) atomic oxygen is the most active site for oxidation, (2) molecular oxygen is the most selective for PO formation, (3) high basicity of the adsorbed oxygen favors AHS, and (4) the active site on the catalyst should be sufficiently electropositive to maintain a weakly basic surface oxygen. In addition to the design principles based on fundamental mechanistic understanding, practical catalyst design also depends on many factors including particle size, surface area, porosity, and supports. In order to overcome these challenges, some of the future opportunities for catalyst design are listed below:

- 1. To design bimetallic or trimetallic catalysts with desired electronic structures that control the oxygen basicity and stabilize the OMC. It has been demonstrated that bimetallic surfaces often show unique properties that are different from their parental metals. The electronic structure of bimetallic alloys can be modified through the ligand effect and strain effect [31]. Using a combination of Cu, Ag, and Au, it is worthy to explore catalyst compositions with an optimal electronic structure to maximize the activity and selectivity of PO production.
- 2. To use an inverse oxide moiety on metal surfaces to enhance the interaction between the substrate and the overlayer and thereby stabilize the active sites. The inverse oxide design can maximize the interaction between the substrate and the overlayer, generating active sites that cannot be stabilized otherwise. It has been shown that a TiO_X layer deposited over the Cu₂O surface can create and stabilize the Cu⁺ species, which serve as the active sites for anchoring the OMC for PO formation [20]. This strategy can potentially be applied to explore other catalytic systems of supporting different oxide (TiO_X, Al₂O₃, etc.) clusters on group IB metal surfaces to design improved interfacial sites for PO formation.
- 3. To use relevant probe molecules to investigate OMC formation, allylic hydrogen abstraction, and epoxide selectivity on these surfaces. For example, previous studies have used 2-iodoethanol and tert-butanol as probe molecules to investigate the epoxidation of ethylene and higher olefins [105,106], and allyl alcohol has been used to study oxidation on Ag(110) [107]. This idea can be expanded by using C3 alcohols and halogenated probe molecules to study propylene epoxidation selectivity.
- 4. To verify the key intermediates using multiple ex-situ and insitu characterization techniques. Vibrational spectroscopy has been used to identify the formation of the OMC on the TiCuO_x mixed oxide surface by comparing experimentally measured and DFT-calculated vibrational frequencies of surface intermediates. XPS and NEXAFS have been employed to provide additional information on the adsorbed species as well as the oxidation states of metals. The structure of the surfaces and interfacial sites can be characterized using STM. The combination of these techniques should be used, whenever possible, to explore new catalytic surfaces. In addition, NEXAFS measurements can be performed under non-UHV conditions using the fluorescence-yield method [62]. Finally, studies on model surfaces should be closely coupled with in-situ X-ray absorption and diffraction measurements [108] of the relevant powder catalysts under reaction conditions for propylene epoxidation.
- 5. To understand the effect of promoters on epoxidation selectivity. Several patents have reported increased selectivity on Agbased catalysts for propylene epoxidation including modification of Ag catalysts with alkali, alkaline earth, and halogen

- promoters [109]. Experimental and theoretical studies of the effects of promoters should provide useful guidance on the design of more selective catalysts for propylene epoxidation.
- 6. To accelerate the identification of promising catalytic structures using DFT and machine learning. Because there are many potential multi-metallic surface structures and oxide/metal interfacial sites, the computational expense associated with DFT calculations is too high for the screening of a large number of candidates. Recent advances have shown that machine learning can be used to significantly accelerate first-principle DFT calculations. This is accomplished by using DFT-computed reaction energetics and adsorbate binding configurations as input to train machine learning models [110]. For example, several recent papers have used machine learning to understand complex reaction networks [111], predict catalyst properties [112], and discover new catalysts [113]. The same strategy can be applied to guide catalyst design for propylene epoxidation.

Acknowledgements

This work has been supported by the NSF DMREF program under grant number CBET1921946.

References

- [1] S.J. Khatib, S.T. Oyama, Direct oxidation of propylene to propylene oxide with molecular oxygen: a review, Catal. Rev. 57 (2015) 306—344, https://doi.org/ 10.1080/01614940.2015.1041849.
- [2] A.H. Tullo, P.L. Short, Propylene oxide routes take off, Chem. Eng. News 84 (2006) 22–23, https://doi.org/10.1021/cen-v084n041.p022.
- [3] T.E. Lefort, Process for the Production of Ethylene Oxide, 1935, 1998878.
- [4] G.A. Cook, Production of Propylene Oxide, 1947, p. 2530509.
- [5] S. Linic, M.A. Barteau, Control of ethylene epoxidation selectivity by surface oxametallacycles, J. Am. Chem. Soc. 125 (2003) 4034–4035, https://doi.org/ 10.1021/ja029076g.
- [6] S. Linic, M.A. Barteau, Construction of a reaction coordinate and a microkinetic model for ethylene epoxidation on silver from DFT calculations and surface science experiments, J. Catal. 214 (2003) 200–212, https://doi.org/ 10.1016/S0021-9517(02)00156-2.
- [7] S. Linic, M.A. Barteau, On the mechanism of Cs promotion in ethylene epoxidation on Ag, J. Am. Chem. Soc. 126 (2004) 8086–8087, https://doi.org/ 10.1021/ja048462q.
- [8] S. Linic, H. Piao, K. Adib, M.A. Barteau, Ethylene epoxidation on Ag: identification of the crucial surface intermediate by experimental and theoretical investigation of its electronic structure, Angew. Chem. Int. Ed. 43 (2004) 2918–2921, https://doi.org/10.1002/anie.200353584.
- [9] M.L. Bocquet, A. Michaelides, D. Loffreda, P. Sautet, A. Alavi, D.A. King, New insights into ethene epoxidation on two oxidized Ag{111} surfaces, J. Am. Chem. Soc. 125 (2003) 5620–5621, https://doi.org/10.1021/ja0297741.
- [10] P. Christopher, S. Linic, Engineering selectivity in heterogeneous catalysis: Ag nanowires as selective ethylene epoxidation catalysts, J. Am. Chem. Soc. 130 (2008) 11264–11265, https://doi.org/10.1021/ja803818k.
- [11] X. Liu, R.J. Madix, C.M. Friend, Unraveling molecular transformations on surfaces: a critical comparison of oxidation reactions on coinage metals, Chem. Soc. Rev. 37 (2008) 2243–2261, https://doi.org/10.1039/b800309m.
- [12] R.M. Lambert, F.J. Williams, R.L. Cropley, A. Palermo, Heterogeneous alkene epoxidation: past, present and future, J. Mol. Catal. Chem. 228 (2005) 27–33, https://doi.org/10.1016/j.molcata.2004.09.077.
- [13] T.A. Nijhuis, M. Makkee, J.A. Moulijn, B.M. Weckhuysen, The production of propene oxide: catalytic processes and recent developments, Ind. Eng. Chem. Res. 45 (2006) 3447–3459, https://doi.org/10.1021/ie0513090.
- [14] G.S. Jones, M. Mavrikakis, M.A. Barteau, J.M. Vohs, First synthesis, experimental and theoretical vibrational spectra of an oxametallacycle on a metal surface, J. Am. Chem. Soc. 120 (1998) 3196–3204, https://doi.org/10.1021/ja973609h.
- [15] A. Pulido, P. Concepción, M. Boronat, A. Corma, Aerobic epoxidation of propene over silver (111) and (100) facet catalysts, J. Catal. 292 (2012) 138–147, https://doi.org/10.1016/j.jcat.2012.05.006.
- [16] C.Y. Syu, H.W. Yang, F.H. Hsu, J.H. Wang, The chemical origin and catalytic activity of coinage metals: from oxidation to dehydrogenation, Phys. Chem. Chem. Phys. 16 (2014) 7481–7490, https://doi.org/10.1039/c3cp55477e.
- [17] N. Saliba, D.H. Parker, B.E. Koel, Adsorption of oxygen on Au(111) by exposure to ozone, Surf. Sci. 410 (1998) 270–282, https://doi.org/10.1016/S0039-6028(98)00309-4.
- [18] X. Deng, B.K. Min, A. Guloy, C.M. Friend, Enhancement of O₂ dissociation on Au(111) by adsorbed oxygen: implications for oxidation catalysis, J. Am. Chem. Soc. 127 (2005) 9267–9270, https://doi.org/10.1021/ja050144j.

- [19] B.K. Min, C.M. Friend, Heterogeneous gold-based catalysis for green chemistry: low-temperature CO oxidation and propene oxidation, Chem. Rev. 107 (2007) 2709–2724, https://doi.org/10.1021/cr050954d.
- [20] X. Yang, S. Kattel, K. Xiong, K. Mudiyanselage, S. Rykov, S.D. Senanayake, J.A. Rodriguez, P. Liu, D.J. Stacchiola, J.G. Chen, Direct epoxidation of propylene over stabilized Cu⁺ surface sites on titanium-modified Cu₂O, Angew. Chem. Int. Ed. 54 (2015) 11946–11951, https://doi.org/10.1002/ anie.201504538.
- [21] F. Besenbacher, J.K. Nørskov, Oxygen chemisorption on metal surfaces: general trends for Cu, Ni and Ag, Prog. Surf. Sci. 44 (1993) 5–66, https://doi.org/10.1016/0079-6816(93)90006-H.
- [22] V.v. Kaichev, V.I. Bukhtiyarov, M. Hävecker, A. Knop-Gercke, R.W. Mayer, R. Schlögl, The nature of electrophilic and nucleophilic oxygen adsorbed on silver, Kinet. Catal. 44 (2003) 432–440, https://doi.org/10.1023/A: 1024459305551.
- [23] Y. Xu, J. Greeley, M. Mavrikakis, Effect of subsurface oxygen on the reactivity of the Ag(111) surface, J. Am. Chem. Soc. 127 (2005) 12823–12827, https:// doi.org/10.1021/ja043727m.
- [24] M.M. Montemore, M.A. van Spronsen, R.J. Madix, C.M. Friend, O₂ activation by metal surfaces: implications for bonding and reactivity on heterogeneous catalysts, Chem. Rev. 118 (2018) 2816–2862, https://doi.org/10.1021/ acs.chemrev.7b00217.
- [25] L.A. Cramer, Y. Liu, P. Deshlahra, E.C.H. Sykes, Dynamic restructuring induced oxygen activation on AgCu near-surface alloys, J. Phys. Chem. Lett. 11 (2020) 5844–5848, https://doi.org/10.1021/acs.jpclett.0c00887.
- [26] X. Liu, C.M. Friend, Competing epoxidation and allylic hydrogen activation: trans-β-methylstyrene oxidation on Au(111), J. Phys. Chem. C 114 (2010) 5141–5147, https://doi.org/10.1021/jp9121529.
- [27] R.L. Cropley, F.J. Williams, A.J. Urquhart, O.P.H. Vaughan, M.S. Tikhov, R.M. Lambert, Efficient epoxidation of a terminal alkene containing allylic hydrogen atoms: trans-methylstyrene on Cu{111}, J. Am. Chem. Soc. 127 (2005) 6069–6076, https://doi.org/10.1021/ja042758e.
- [28] J.G. Chen, NEXAFS investigations of transition metal oxides, nitrides, carbides, sulfides and other interstitial compounds, Surf. Sci. Rep. 30 (1997) 1–152, https://doi.org/10.1016/S0167-5729(97)00011-3.
- [29] A. Kuznetsova, I. Popova, J.T. Yates, M.J. Bronikowski, C.B. Huffman, J. Liu, R.E. Smalley, H.H. Hwu, J.G. Chen, Oxygen-containing functional groups on single-wall carbon nanotubes: NEXAFS and vibrational spectroscopic studies, J. Am. Chem. Soc. 123 (2001) 10699–10704, https://doi.org/10.1021/ja011021b.
- [30] X. Deng, B.K. Min, X. Liu, C.M. Friend, Partial oxidation of propene on oxygencovered Au(111), J. Phys. Chem. B 110 (2006) 15982–15987, https://doi.org/ 10.1021/jp062305r.
- [31] J.G. Chen, C.A. Menning, M.B. Zellner, Monolayer bimetallic surfaces: experimental and theoretical studies of trends in electronic and chemical properties, Surf. Sci. Rep. 63 (2008) 201–254, https://doi.org/10.1016/ j.surfrep.2008.02.001.
- [32] D. Düzenli, D.O. Atmaca, M.G. Gezer, I. Onal, A density functional theory study of partial oxidation of propylene on $Cu_2O(001)$ and CuO(001) surfaces, Appl. Surf. Sci. 355 (2015) 660–666, https://doi.org/10.1016/j.apsusc.2015.07.155.
- [33] T.A. Baker, B. Xu, S.C. Jensen, C.M. Friend, E. Kaxiras, Role of defects in propene adsorption and reaction on a partially O-covered Au(111) surface, Catal. Sci. Technol. 1 (2011) 1166–1174, https://doi.org/10.1039/c1cy00076d.
- [34] Y.Y. Song, G.C. Wang, Theoretical study of propylene epoxidation over Cu₂O(111) surface: activity of O, O, and O₂ species, J. Phys. Chem. C 122 (2018) 21500–21513, https://doi.org/10.1021/acs.jpcc.8b07044.
- [35] J. Huang, M. Haruta, Gas-phase propene epoxidation over coinage metal catalysts, Res. Chem. Intermed. 38 (2012) 1–24, https://doi.org/10.1007/ s11164-011-0424-6.
- [36] K.A. Davis, D.W. Goodman, Propene adsorption on clean and oxygen-covered Au(111) and Au(100) surfaces, J. Phys. Chem. B 104 (2000) 8557–8562, https://doi.org/10.1021/jp001699y.
- [37] G. Sun, Y. Jin, Z. Wang, H. Xu, P. Chai, W. Huang, Site- and surface species-dependent propylene oxidation with molecular oxygen on gold surface, Chin. Chem. Lett. 29 (2018) 1883–1887, https://doi.org/10.1016/j.cclet.2018.10.027.
- [38] W. Huang, Z. Jiang, J.M. White, Distinct oxidation behaviors of π-bonded and di-σ-bonded propylene on Ag(1 1 1), Catal. Today 131 (2008) 360–366, https://doi.org/10.1016/j.cattod.2007.10.045.
- [39] W.X. Huang, J.M. White, Propene adsorption on Ag(1 1 1): a TPD and RAIRS study, Surf. Sci. 513 (2002) 399–404, https://doi.org/10.1016/S0039-6028(02)01810-1.
- [40] W.X. Huang, J.M. White, Transition from π-bonded to di-σ metallacyclic propene on o-modified Ag(111), Langmuir 18 (2002) 9622–9624, https://doi.org/10.1021/la026089z.
- [41] W.X. Huang, J.M. White, Propene oxidation on Ag(111): spectroscopic evidence of facile abstraction of methyl hydrogen, Catal. Lett. 84 (2002) 143–146, https://doi.org/10.1023/A:1021471718608.
- [42] J.T. Roberts, R.J. Madix, W.W. Crew, The rate-limiting step for olefin combustion on silver: experiment compared to theory, J. Catal. 141 (1993) 300–307, https://doi.org/10.1006/jcat.1993.1137.
- [43] M.A. Barteau, R.J. Madix, Low-pressure oxidation mechanism and reactivity of propylene on Ag(110) and relation to gas-phase acidity, J. Am. Chem. Soc. 105 (1983) 344–349, https://doi.org/10.1021/ja00341a008.

- [44] J.T. Ranney, S.R. Bare, The reaction of propylene with ordered and disordered oxygen atoms adsorbed on the Ag(110) surface, Surf. Sci. 382 (1997) 266–274, https://doi.org/10.1016/S0039-6028(97)00184-2.
- [45] J. Pawela-Crew, R.J. Madix, The effect of subsurface oxygen on the desorption kinetics of propylene from Ag(110), J. Catal. 153 (1995) 158–164, https:// doi.org/10.1006/jcat.1995.1117.
- [46] J.T. Ranney, J.L. Gland, S.R. Bare, The desorption of propylene oxide from oxygen atom and hydroxyl covered Ag(110), Surf. Sci. 401 (1998) 1–11, https://doi.org/10.1016/S0039-6028(97)00880-7.
- [47] J.L. Solomon, R.J. Madix, J. Stöhr, Orientation of ethylene and propylene on Ag(110) from near edge x-ray adsorption fine structure, J. Chem. Phys. 93 (1990) 8379–8382, https://doi.org/10.1063/1.459269.
- [48] S.R. Bare, Comparison of ethylene oxide and propylene oxide chemisorbed on clean and oxygen precovered Ag(110), J. Vac. Sci. Technol.: Vacuum Surf. Films 10 (1992) 2336–2341, https://doi.org/10.1116/1.577940.
- [49] J.W. Medlin, M.A. Barteau, J.M. Vohs, Oxametallacycle formation via ringopening of 1-epoxy-3-butene on Ag(110): a combined experimental/theoretical approach, J. Mol. Catal. Chem. 163 (2000) 129–145, https://doi.org/ 10.1016/51381-1169/00)00406-4.
- [50] J.W. Medlin, A.B. Sherrill, J.G. Chen, M.A. Barteau, Experimental and theoretical probes of the structure of oxametallacycle intermediates derived from 1-epoxy-3-butene on Ag(110), J. Phys. Chem. B 105 (2001) 3769–3775, https://doi.org/10.1021/jp003389l.
- [51] J.B. Reitz, E.I. Solomon, Propylene oxidation on copper oxide surfaces: electronic and geometric contributions to reactivity and selectivity, J. Am. Chem. Soc. 120 (1998) 11467–11478, https://doi.org/10.1021/ja981579s.
- [52] K.H. Schulz, D.F. Cox, Propene oxidation over Cu₂O single-crystal surfaces: a surface science study of propene activation at 1 atm and 300 K, J. Catal. 143 (1993) 464–480, https://doi.org/10.1006/jcat.1993.1290.
- [53] K.H. Schulz, D.F. Cox, Propene adsorption on Cu₂O single-crystal surfaces, Surf. Sci. 262 (1992) 318–334, https://doi.org/10.1016/0039-6028(92) 90129-T
- [54] F.J. Williams, R.L. Cropley, O.P.H. Vaughan, A.J. Urquhart, M.S. Tikhov, C. Kolczewski, K. Hermann, R.M. Lambert, Critical influence of adsorption geometry in the heterogeneous epoxidation of "allylic" alkenes: structure and reactivity of three phenylpropene isomers on Cu(111), J. Am. Chem. Soc. 127 (2005) 17007—17011, https://doi.org/10.1021/ja055635i.
- [55] R.L. Cropley, F.J. Williams, O.P.H. Vaughan, A.J. Urquhart, M.S. Tikhov, R.M. Lambert, Copper is highly effective for the epoxidation of a "difficult" alkene, whereas silver is not, Surf. Sci. 578 (2005) 1–4, https://doi.org/ 10.1016/j.susc.2005.01.024.
- [56] H.M. Ajo, V.A. Bondzie, C.T. Campbell, Propene adsorption on gold particles on TiO₂(110), Catal. Lett. 78 (2002) 359–368, https://doi.org/10.1023/A: 1014925121945.
- [57] J.J. Cowell, A.K. Santra, R.M. Lambert, Ultraselective epoxidation of butadiene on Cu{111} and the effects of Cs promotion [6], J. Am. Chem. Soc. 122 (2000) 2381–2382, https://doi.org/10.1021/ja994125j.
- [58] M.D. Robbins, M.A. Henderson, The partial oxidation of isobutene and propene on TiO₂(110), J. Catal. 238 (2006) 111–121, https://doi.org/10.1016/j.icat.2005.11.041.
- [59] N.F. Brown, M.A. Barteau, Epoxides as probes of oxametallacycle chemistry on Rh(111), Surf. Sci. 298 (1993) 6–17, https://doi.org/10.1016/0039-6028(93)90075-U.
- [60] X. Xu, C.M. Friend, Partial oxidation without allylic C-H bond activation: the conversion of propene to acetone on Rh(111)-p(2×1)-O, J. Am. Chem. Soc. 113 (1991) 6779–6785, https://doi.org/10.1021/ja00018a010.
- [61] A.M. Gabelnick, J.L. Gland, Propylene deep oxidation on the Pt(1 1 1) surface: temperature programmed studies over extended coverage ranges, Surf. Sci. 440 (1999) 340–350, https://doi.org/10.1016/S0039-6028(99)00684-6.
- [62] A.M. Gabelnick, A.T. Capitano, S.M. Kane, J.L. Gland, D.A. Fischer, Propylene oxidation mechanisms and intermediates using in situ soft X-ray fluorescence methods on the Pt(111) surface, J. Am. Chem. Soc. 122 (2000) 143–149, https://doi.org/10.1021/ja992865m.
- [63] P.J. van den Hoek, Ethylene epoxidation on Ag(110): the role of subsurface oxygen, J. Phys. Chem. 93 (1989) 6469–6475, https://doi.org/10.1021/ j100354a038.
- [64] S. Linic, M.A. Barteau, Formation of a stable surface oxametallacycle that produces ethylene oxide, J. Am. Chem. Soc. 124 (2002) 310–317, https:// doi.org/10.1021/ia0118136.
- [65] T. Hayashi, K. Tanaka, M. Haruta, Selective vapor-phase epoxidation of propylene over Au/TiO₂ catalysts in the presence of oxygen and hydrogen, J. Catal. 178 (1998) 566–575, https://doi.org/10.1006/jcat.1998.2157.
- [66] A.K. Sinha, S. Seelan, S. Tsubota, M. Haruta, Catalysis by gold nanoparticles: epoxidation of propene, Top. Catal. 29 (2004) 95–102, https://doi.org/ 10.1023/b:toca.0000029791.69935.53.
- [67] E.E. Stangland, K.B. Stavens, R.P. Andres, W.N. Delgass, Characterization of gold-titania catalysts via oxidation of propylene to propylene oxide, J. Catal. 191 (2000) 332–347, https://doi.org/10.1006/jcat.1999.2809.
- [68] E. Sacaliuc, A.M. Beale, B.M. Weckhuysen, T.A. Nijhuis, Propene epoxidation over Au/Ti-SBA-15 catalysts, J. Catal. 248 (2007) 235–248, https://doi.org/ 10.1016/j.jcat.2007.03.014.
- [69] S. Linic, P. Christopher, H. Xin, A. Marimuthu, Catalytic and photocatalytic transformations on metal nanoparticles with targeted geometric and plasmonic properties, Acc. Chem. Res. 46 (2013) 1890–1899, https://doi.org/ 10.1021/ar3002393.

- [70] A. Marimuthu, Z. Jianwen, S. Linic, Tuning selectivity in propylene epoxidation by plasmon mediated photo-switching of Cu oxidation state, Science 339 (2013) 1590–1593.
- [71] S. Linic, P. Christopher, Overcoming limitation in the design of selective solid catalysts by manipulating shape and size of catalytic particles: epoxidation reactions on silver, ChemCatChem 2 (2010) 1061–1063, https://doi.org/ 10.1002/cctc.201000163.
- [72] Q. Hua, T. Cao, X.K. Gu, J. Lu, Z. Jiang, X. Pan, L. Luo, W.X. Li, W. Huang, Crystal-plane-controlled selectivity of Cu₂O catalysts in propylene oxidation with molecular oxygen, Angew. Chem. Int. Ed. 53 (2014) 4856–4861, https:// doi.org/10.1002/anje.201402374.
- [73] Q. Wang, C. Zhan, L. Zhou, G. Fu, Z. Xie, Effects of Cl⁻ on Cu₂O nanocubes for direct epoxidation of propylene by molecular oxygen, Catal. Commun. 135 (2020) 105897, https://doi.org/10.1016/j.catcom.2019.105897.
- [74] B. Yu, T. Ayvali, Z.Q. Wang, X.Q. Gong, A.A. Bagabas, S.C.E. Tsang, Gas phase selective propylene epoxidation over La₂O₃-supported cubic silver nanoparticles, Catal. Sci. Technol. 9 (2019) 3435–3444, https://doi.org/10.1039/ c9cy00567f.
- [75] M.F. Fellah, I. Onal, Epoxidation of propylene on a [Ag₁₄O₉] cluster representing Ag₂O (001) surface: a density functional theory study, Catal. Lett. 142 (2012) 22–31, https://doi.org/10.1007/s10562-011-0727-7.
- [76] L.M. Molina, S. Lee, K. Sell, G. Barcaro, A. Fortunelli, B. Lee, S. Seifert, R.E. Winans, J.W. Elam, M.J. Pellin, I. Barke, V. von Oeynhausen, Y. Lei, R.J. Meyer, J.A. Alonso, A. Fraile Rodríguez, A. Kleibert, S. Giorgio, C.R. Henry, K.H. Meiwes-Broer, S. Vajda, Size-dependent selectivity and activity of silver nanoclusters in the partial oxidation of propylene to propylene oxide and acrolein: a joint experimental and theoretical study, Catal. Today 160 (2011) 116–130, https://doi.org/10.1016/j.cattod.2010.08.022.
- [77] I. Tezsevin, R.A. van Santen, I. Onal, A density functional theory study of propylene epoxidation mechanism on Ag₂O(001) surface, Phys. Chem. Chem. Phys. 20 (2018) 26681–26687, https://doi.org/10.1039/c8cp04210a.
- [78] L.M. Molina, M.J. López, J.A. Alonso, Ab initio studies of propene epoxidation on oxidized silver surfaces, Phys. Chem. Chem. Phys. 16 (2014) 26546–26552, https://doi.org/10.1039/c4cp02103g.
- [79] M. Boronat, A. Pulido, P. Concepción, A. Corma, Propene epoxidation with O₂ or H₂-O₂ mixtures over silver catalysts: theoretical insights into the role of the particle size, Phys. Chem. Chem. Phys. 16 (2014) 26600–26612, https://doi.org/10.1039/c4cp02198c.
- [80] A. Kulkarni, M. Bedolla-Pantoja, S. Singh, R.F. Lobo, M. Mavrikakis, M.A. Barteau, Reactions of propylene oxide on supported silver catalysts: insights into pathways limiting epoxidation selectivity, Top. Catal. 55 (2012) 3–12, https://doi.org/10.1007/s11244-012-9773-7.
- [81] Y. Dai, Z. Chen, Y. Guo, G. Lu, Y. Zhao, H. Wang, P. Hu, Significant enhancement of the selectivity of propylene epoxidation for propylene oxide: a molecular oxygen mechanism, Phys. Chem. Chem. Phys. 19 (2017) 25129–25139, https://doi.org/10.1039/c7cp02892j.
- [82] L. Cheng, C. Yin, F. Mehmood, B. Liu, J. Greeley, S. Lee, B. Lee, S. Seifert, R.E. Winans, D. Teschner, R. Schlögl, S. Vajda, L.A. Curtiss, Reaction mechanism for direct propylene epoxidation by alumina-supported silver aggregates: the role of the particle/support interface, ACS Catal. 4 (2014) 32–39, https://doi.org/10.1021/cs4009368.
- [83] A. Roldan, D. Torres, J.M. Ricart, F. Illas, On the effectiveness of partial oxidation of propylene by gold: a density functional theory study, J. Mol. Catal. Chem. 306 (2009) 6–10, https://doi.org/10.1016/ j.molcata.2009.02.013.
- [84] Q. Zhang, X. Zhao, J. Yang, M. Zheng, W. Fan, Theoretical insights into propene epoxidation on Au₇/anatase TiO_{2-x}(001) catalysts: effect of the interface and reaction atmosphere, J. Phys. Chem. C 123 (2019) 3568–3578, https://doi.org/10.1021/acs.jpcc.8b11201.
- [85] L.v. Moskaleva, Theoretical mechanistic insights into propylene epoxidation on Au-based catalysts: surface O versus OOH as oxidizing agents, Catal. Today 278 (2016) 45–55, https://doi.org/10.1016/j.cattod.2016.05.034.
- [86] S. Lee, L.M. Molina, M.J. López, J.A. Alonso, B. Hammer, B. Lee, S. Seifert, R.E. Winans, J.W. Elam, M.J. Pellin, S. Vajda, Selective propene epoxidation on immobilized Au₆₋₁₀ clusters: the effect of hydrogen and water on activity and selectivity, Angew. Chem. Int. Ed. 48 (2009) 1467–1471, https://doi.org/ 10.1002/anie.200804154.
- [87] A.C. Kizilkaya, S. Senkan, I. Onal, Investigation of ruthenium-copper bimetallic catalysts for direct epoxidation of propylene: a DFT study, J. Mol. Catal. Chem. 330 (2010) 107–111, https://doi.org/10.1016/j.molcata.2010.07.008.
- [88] Y.Y. Song, G.C. Wang, A DFT study and microkinetic simulation of propylene partial oxidation on CuO (111) and CuO (100) surfaces, J. Phys. Chem. C 120 (2016) 27430–27442, https://doi.org/10.1021/acs.jpcc.6b09621.
- [89] D. Torres, N. Lopez, F. Illas, R.M. Lambert, Low-basicity oxygen atoms: a key in the search for propylene epoxidation catalysts, Angew. Chem. Int. Ed. 46 (2007) 2055–2058, https://doi.org/10.1002/anie.200603803.
- [90] Y. Song, B. Dong, S. Wang, Z. Wang, M. Zhang, P. Tian, G. Wang, Z. Zhao, Selective oxidation of propylene on Cu₂O(111) and Cu₂O(110) surfaces: a systematically DFT study, ACS Omega 5 (2020) 6260–6269, https://doi.org/ 10.1021/acsomega.9b02997.
- [91] J.W. Medlin, M. Mavrikakis, M.A. Barteau, Stabilities of substituted oxametallacycle intermediates: implications for regioselectivity of epoxide ring opening and olefin epoxidation, J. Phys. Chem. B 103 (1999) 11169–11175, https://doi.org/10.1021/jp992812r.
- [92] D.O. Atmaca, D. Düzenli, M.O. Ozbek, I. Onal, A density functional theory

- study of propylene epoxidation on RuO₂(110) surface, Appl. Surf. Sci. 385 (2016) 99–105, https://doi.org/10.1016/j.apsusc.2016.05.090.
- [93] C. Chang, Y. Wang, J. Li, Theoretical investigations of the catalytic role of water in propene epoxidation on gold nanoclusters: a hydroperoxylmediated pathway, Nano Research 4 (2011) 131–142, https://doi.org/ 10.1007/s12274-010-0083-8.
- [94] J. García-Aguilar, I. Miguel-García, J. Juan-Juan, I. Such-Basáñez, E.S. Fabián, D. Cazorla-Amorós, One step-synthesis of highly dispersed iron species into silica for propylene epoxidation with dioxygen, J. Catal. 338 (2016) 154–167, https://doi.org/10.1016/j.jcat.2016.03.004.
- [95] A.M. Joshi, W.N. Delgass, K.T. Thomson, Partial oxidation of propylene to propylene oxide over a neutral gold trimer in the gas phase: a density functional theory study, J. Phys. Chem. B 110 (2006) 2572–2581, https:// doi.org/10.1021/ip054809f.
- [96] H. Munakata, Y. Oumi, A. Miyamoto, A DFT study on peroxo-complex in titanosilicate catalyst: hydrogen peroxide activation on titanosilicalite-1 catalyst and reaction mechanisms for catalytic olefin epoxidation and for hydroxylamine formation from ammonia, J. Phys. Chem. B 105 (2001) 3493—3501, https://doi.org/10.1021/jp0022196.
- [97] D.H. Wells, A.M. Joshi, W.N. Delgass, K.T. Thomson, A quantum chemical study of comparison of various propylene epoxidation mechanisms using H₂O₂ and TS-1 catalyst, J. Phys. Chem. B 110 (2006) 14627–14639, https:// doi.org/10.1021/jp062368.
- [98] X. Nie, X. Ji, Y. Chen, X. Guo, C. Song, Mechanistic investigation of propylene epoxidation with H₂O₂ over TS-1: active site formation, intermediate identification, and oxygen transfer pathway, Mol. Catal. 441 (2017) 150–167, https://doi.org/10.1016/j.mcat.2017.08.011.
- [99] D.H. Wells, W.N. Delgass, K.T. Thomson, Evidence of defect-promoted reactivity for epoxidation of propylene in titanosilicate (TS-1) catalysts: a DFT study, J. Am. Chem. Soc. 126 (2004) 2956–2962, https://doi.org/10.1021/ja037741v.
- [100] R.R. Sever, T.W. Root, DFT study of solvent coordination effects on titanium-based epoxidation catalysts. part one: formation of the titanium hydroperoxo intermediate, J. Phys. Chem. B 107 (2003) 4080–4089, https://doi.org/10.1021/jp026056s.
- [101] R.R. Sever, T.W. Root, DFT study of solvent coordination effects on titanium-based epoxidation catalysts. part two: reactivity of titanium hydroperoxo complexes in ethylene epoxidation, J. Phys. Chem. B 107 (2003) 4090–4099, https://doi.org/10.1021/jp026057k.
- [102] R.D. Bach, M.N. Glukhovtsev, C. Gonzalez, M. Marquez, C.M. Estévez, A.G. Baboul, H.B. Schlegel, Nature of the transition structure for alkene

- epoxidation by peroxyformic acid, dioxirane, and dimethyldioxirane: a comparison of B3LYP density functional theory with higher computational levels, J. Phys. Chem. 101 (1997) 6092–6100, https://doi.org/10.1021/jp970378s.
- [103] M. Freccero, R. Gandolfi, M. Sarzi-Amadè, A. Rastelli, DFT computational study of the epoxidation of olefins with dioxiranes, Tetrahedron 54 (1998) 6123–6134, https://doi.org/10.1016/S0040-4020(98)00305-6.
- [104] Z. Wan, Z. Lin, J. Peng, W. Chen, X. Li, X. Chen, Theoretical study of propylene epoxidation heterogeneous-homogeneous mechanism over MoO_x/SiO₂ catalyst, Int. J. Quant. Chem. 120 (2020) 1–15, https://doi.org/10.1002/ qua.26328.
- [105] S. Linic, J.W. Medlin, M.A. Barteau, Synthesis of oxametallacycles from 2iodoethanol on Ag(111) and the structure dependence of their reactivity, Langmuir 18 (2002) 5197–5204, https://doi.org/10.1021/la011783k.
- [106] R.L. Brainard, R.J. Madix, Enhanced stability of t-butanol reaction intermediates on oxygen covered Cu(110): cleavage of unactivated C-H bonds on metal surfaces, Surf. Sci. 214 (1989) 396–406.
- [107] R.L. Brainard, C.G. Peterson, R.J. Madix, Surface-mediated isomerization and oxidation of allyl alcohol on Cu(110), J. Am. Chem. Soc. 111 (1989) 4553–4561, https://doi.org/10.1021/ja00195a003.
- [108] A.I. Frenkel, J.A. Rodriguez, J.G. Chen, Synchrotron techniques for in situ catalytic studies: capabilities, challenges, and opportunities, ACS Catal. 2 (2012) 2269–2280, https://doi.org/10.1021/cs3004006.
- [109] J.R. Monnier, The direct epoxidation of higher olefins using molecular oxygen, Appl. Catal. Gen. 221 (2001) 73–91, https://doi.org/10.1016/S0926-860X(01)00799-2.
- [110] N. Artrith, Z. Lin, J.G. Chen, Predicting the activity and selectivity of bimetallic metal catalysts for ethanol reforming using machine learning, ACS Catal. 10 (2020) 9438–9444, https://doi.org/10.1021/acscatal.0c02089.
- [111] Z.W. Ulissi, A.J. Medford, T. Bligaard, J.K. Nørskov, To address surface reaction network complexity using scaling relations machine learning and DFT calculations, Nat. Commun. 8 (2017) 14621, https://doi.org/10.1038/ncomms14621.
- [112] J.R. Kitchin, Machine learning in catalysis, Nat. Catal. 1 (2018) 230–232, https://doi.org/10.1038/s41929-018-0056-y.
- [113] M. Zhong, K. Tran, Y. Min, C. Wang, Z. Wang, C.T. Dinh, P. de Luna, Z. Yu, A.S. Rasouli, P. Brodersen, S. Sun, O. Voznyy, C.S. Tan, M. Askerka, F. Che, M. Liu, A. Seifitokaldani, Y. Pang, S.C. Lo, A. Ip, Z. Ulissi, E.H. Sargent, Accelerated discovery of CO₂ electrocatalysts using active machine learning, Nature 581 (2020) 178–183, https://doi.org/10.1038/s41586-020-2242-8.